

## **NFATc1 promotes anti-tumoral effector functions and memory CD8<sup>+</sup> T cell differentiation during non-small cell lung cancer development**

Lisanne Heim<sup>1</sup>, Juliane Friedrich<sup>1</sup>, Marina Engelhardt<sup>1</sup>, Denis I. Trufa<sup>2</sup>, Carol I. Geppert<sup>3</sup>, Ralf J. Rieker<sup>3</sup>, Horia Sirbu<sup>2</sup> and Susetta Finotto<sup>1\*</sup>

<sup>1</sup>Department of Molecular Pneumology, University Hospital, Friedrich-Alexander-Universität Erlangen-Nürnberg, Erlangen, Germany

<sup>2</sup>Department of Thoracic Surgery, University Hospital, Friedrich-Alexander-Universität Erlangen-Nürnberg, Erlangen, Germany

<sup>3</sup>Institute of Pathology, University Hospital, Friedrich-Alexander-Universität Erlangen-Nürnberg, Erlangen, Germany

**Running title:** NFATc1 promotes anti-tumoral T cell functions in NSCLC

**Keywords:** Non-Small Cell Lung Cancer (NSCLC), NFATc1, IL-2, memory CD8<sup>+</sup> T cells, αPD-1 immunotherapy

\*Corresponding author

Prof. Susetta Finotto, PhD

Laboratories of Cellular and Molecular Lung Immunology

Department of Molecular Pneumology

Friedrich-Alexander-Universität Erlangen-Nürnberg

Hartmannstraße 14

91052 Erlangen, Germany

Phone: 0049-9131-8542454

Fax: 0049-9131-8535981

Email: [Susetta.Finotto@uk-erlangen.de](mailto:Susetta.Finotto@uk-erlangen.de)

**Competing financial interest statement:** All authors declare no conflict of interest on the matter described in this manuscript.

**Total number of figures and tables:** 6+1 (+3 supplementary figures, +2 supplementary Tables)

## Abstract

Nuclear factor of activated T cells 1 (NFATc1) is a transcription factor activated by T cell receptor (TCR) and  $\text{Ca}^{2+}$ -signaling that affects T cell activation and effector function. Upon tumor antigen challenge, TCR and calcium-release-activated channels are induced, promoting NFAT dephosphorylation and translocation into the nucleus. In this study, we report a progressive decrease of NFATc1 in lung tumor tissue and in tumor-infiltrating lymphocytes (TIL) of patients suffering from advanced stage non-small cell lung cancer (NSCLC). Mice harboring conditionally inactivated NFATc1 in T cells (NFATc1<sup>ΔCD4</sup>) showed increased lung tumor growth associated with impaired T cell activation and function. Furthermore, in the absence of NFATc1, reduced IL-2 influenced the development of memory CD8<sup>+</sup> T cells. We found a reduction of effector memory and CD103<sup>+</sup> tissue-resident memory (TRM) T cells in the lung of tumor-bearing NFATc1<sup>ΔCD4</sup> mice, underlining an impaired cytotoxic T cell response and a reduced TRM tissue-homing capacity. In CD4<sup>+</sup>ICOS<sup>+</sup> T cells, programmed cell death 1 (PD-1) was induced in the draining lymph nodes of these mice and associated with lung tumor cell growth. Targeting PD-1 resulted in NFATc1 induction in CD4<sup>+</sup> and CD8<sup>+</sup> T cells in tumor-bearing mice and was associated with increased anti-tumor cytotoxic functions. This study reveals a role of NFATc1 in the activation and cytotoxic functions of T cells, in the development of memory CD8<sup>+</sup> T cell subsets, and in the regulation of T cell exhaustion. These data underline the indispensability of NFATc1 for successful anti-tumor immune responses in NSCLC patients.

**Significance:** The multi-faceted role of NFATc1 in the activation and function of T cells during lung cancer development make it a critical participant in anti-tumor immune responses in NSCLC patients.

## Introduction

Nuclear factor of activated T-cells is a transcription factor family that consists of five members, among which NFAT1-4 (NFATc1-NFATc4) are regulated by  $\text{Ca}^{2+}$ -calcineurin signaling. NFATc1 and NFATc2 are the main isoforms expressed in T-cells critical in regulating early gene transcription in response to T-cell receptor (TCR)-mediated signals [1-3]. In resting T-cells, NFAT transcription factors are located in the cytosol in an inactive, phosphorylated state. Upon TCR stimulation, NFAT is activated by calcium flux released from the endoplasmic reticulum and the extracellular environment through store-operated channels. Induced intracytoplasmic calcium promotes calmodulin, a calcium sensor protein which activates the phosphatase calcineurin. Calcineurin dephosphorylates NFAT resulting in its translocation into the nucleus where it cooperates with other transcription factors promoting cell specific gene transcription [3, 4].

The expression of NFATc1 in T-cells is initiated by two distinct promoters, resulting along with alternative splice/polyadenylation events in six isoforms: NFATc1 $\alpha$ A-C and NFATc1 $\beta$ A-C [5, 6]. NFATc1 $\alpha$ A has been shown to be strongly induced following TCR stimulation and is maintained by a positive autoregulation which enables a massive synthesis and facilitates T-cells to exert effector functions and escape from apoptosis [5, 7-9]. Cytotoxic effector functions are mediated by CD8<sup>+</sup> T-cells via the secretion of inflammatory cytokines [10, 11]. A recent study described that NFATc1-deficient cytotoxic T-cells showed reduced cytotoxicity against tumour cells. Furthermore, transcriptome analysis demonstrates diminished RNA levels of numerous genes in NFATc1<sup>-/-</sup> CD8<sup>+</sup> T-cells, including *Il2* [9]. Interleukin-2 (IL-2) is one of the first molecules that has been shown to be induced by NFATc1 [12] and is important for T-cell activation, proliferation and survival [13, 14]. Furthermore, IL-2 influences the generation of memory CD8<sup>+</sup> T-cells classified into central memory (TCM), effector memory (TEM) and tissue-resident memory (TRM) CD8<sup>+</sup> T-cells that differ in their tissue homing capacity and effector functions [13, 15-17]. In most of the established tumours, tumour-infiltrating lymphocytes (TILs) are found to be exhausted leading to cancer immune evasion. One remarkable feature of functionally exhausted T-cells is the expression of inhibitory checkpoint receptors which desensitize TCR

signaling leading to functional impairment of T-cell activation. Based on these findings, cancer immunotherapies have been developed that reactivate exhausted TILs by blocking inhibitory checkpoint receptors [18-20]. Programmed cell death (PD)-1 is one of the most successful checkpoint target in different cancer types including non-small cell lung cancer (NSCLC). Nevertheless, only ~30% of patients are responsive to this therapy, and there is a need to find alternate regulators to improve present approaches [19-23]. NFATc1 has been shown to induce the expression of PD-1 upon T-cell activation [24]. But there is still a contradiction regarding the influence of  $\alpha$ PD-1 antibody treatment on NFATc1 in T-cells. Triggering of PD-1 by its ligand PD-L1 expressed on tumour cells induces the inhibition of the phosphatidylinositol-3-kinase (PI3K)/Akt pathway. Akt normally negatively regulates the glycogen-synthase kinase 3 (GSK3) which inhibits NFATc1 [3, 25, 26]. Blocking PD-1 by  $\alpha$ PD-1 antibodies restores TCR signaling and ensured the activation of Akt which inhibits GSK3 and promotes the activation of NFATc1 which induces T-cell activation and effector functions [7, 9, 25]. Thus, NFATc1 could be a key regulator in  $\alpha$ PD-1 anti-cancer immunotherapy.

Here we demonstrate an important function of NFATc1 for successful T-cell mediated anti-tumoural immune responses in the setting of NSCLC. Targeted deletion of NFATc1 in T-cells (NFATc1 <sup>$\Delta$ CD4</sup>) induced increased lung tumour growth in mice associated with impaired T-cell activation and function. In the absence of NFATc1, reduced IL-2 influenced the development of memory CD8<sup>+</sup> T-cells. Consistently, we found a reduction of TEM and CD103<sup>+</sup> TRM T-cells in the lung of tumour-bearing NFATc1 <sup>$\Delta$ CD4</sup> mice underlining an impaired cytotoxic T-cell response and a reduced TRM tissue-homing capacity. PD-1 was found co-expressed and accumulated with CD4<sup>+</sup>ICOS<sup>+</sup> T-cells in the draining lymph nodes (dLN) of NFATc1 <sup>$\Delta$ CD4</sup> and associated with lung tumour cell growth. Moreover, targeting PD1 induced significantly NFATc1 in T-cells accompanied by increased anti-tumour cytotoxic functions. Thus, this study revealed a role of NFATc1 not only in the activation and cytotoxic functions of T-cells, but also in the development of memory CD8<sup>+</sup> T-cell subsets and the regulation of T-cell exhaustion underlining the indispensability of NFATc1 for successful anti-tumour immune responses in NSCLC.

## **Materials and Methods**

### **Human subjects and study population**

This study was performed at the Friedrich-Alexander-University of Erlangen in Germany and was approved by the ethics review board of the University of Erlangen (Re-No: 56\_12B; DRKS-ID: DRKS00005376). Fifty-eight patients that suffered from NSCLC underwent surgery and gave their approval to be enrolled in this study in an informed written consent. The patient studies were conducted in accordance with the ethical guidelines of the Declaration of Helsinki.

The diagnosis of lung cancer was based on pathological confirmation. The histological types of lung cancer were classified according to the classification of the World Health Organization (WHO), formulated in 2004. The staging of lung cancer was based on the Cancer TNM Staging Manual, formulated by the International Association for the Study of Lung Cancer (IASLC) in 2010. During surgery, lung tissue samples were taken from the tumoural area (TU: solid tumour tissue), the peri-tumoural area (PT: up to 2 cm away from the solid tumour) and from the tumour free control area (CTR: >5cm away from the solid tumour). This cohort of NSCLC patients was previously described [27].

### **Protein Extraction and Western blot analyzes**

For protein extraction, lung tissue samples were lysed in RIPA buffer (Thermo Fisher Scientific, Waltham, MA, USA) with added inhibitor cocktail (Roche Diagnostics, Mannheim, Germany), followed by homogenization using the SpeedMill PLUS (Analytik Jena, Jena, Germany) and innuSPEED lysis Tube P (Analytik Jena). After centrifugation (5 min, 3000 r.p.m., 4°C), supernatants were incubated on ice for 45 min, followed by centrifugation (1x 5 min, 3000 r.p.m., 4°C; 1x 45 min, full speed, 4°C). Finally, protein concentration was calculated after using Bradford Assay (Protein Assay Dye Reagent Concentration, Bio-Rad, Munich, Germany). Western blot analysis to detect NFATc1 (1:250; sc-1149, Santa Cruz, Heidelberg, Germany), pNFATc1 (1:250; sc-32978, Santa Cruz) and  $\beta$ -Actin (1:500, sc-1616, Santa Cruz) was performed as previously described [28] with 50  $\mu$ g of total lung protein. Quantification of total NATc1 and pNFATc1 was

performed using the AlphaView Software for FluorChem Systems (Biozym Scientific, Oldendorf, Germany).

### **Double immunohistochemistry (IHC) of NFATc1 and CD3 on paraffin-embedded lung tissue sections**

Immunohistochemistry was performed on paraffin-embedded sections. Before staining, paraffin was removed from the slides by incubation at 72°C for 30 min and treatment with Roti-Histol (Carl Roth, Karlsruhe, Germany) two times for 10 min. The tissue sections were then rehydrated by immersion in ethanol-series with descending concentrations (100%, 95%, 70%) for 3 min each and in deionised water for 1 min, followed by blocking endogeneous peroxidase in 3% H<sub>2</sub>O<sub>2</sub> (in methanol) for 20 min. Heat-induced antigen retrieval was performed as previously described [27] using 1 mM Tris-EDTA wash buffer. Afterwards, slides were incubated with primary antibody to CD3 (1:100, RBK024, Zytomed Systems GmbH, Berlin, Germany) overnight at 4°C. After different washing steps and detection of the primary antibody following the manufacture instructions of the ZytoChem-Plus AP Polymer Kit (POLAP006, Zytomed Systems GmbH) the second antibody to NFATc1 (1:50, sc-7294, Santa Cruz) was applied for 2h at RT. The second antibody was detected following the manufacture instructions of the Dako EnVision Detection System Kit (K4065, Hamburg, Germany). Slides were covered with coverslips using Aquatex (108562, Merck, Darmstadt, Germany). Negative controls were not treated with the primary antibodies, the other steps remain the same. Stained slides were scanned using the digital slide scanner (Scan 150, 3D Histech Ltd, Budapest, Hungary) and NFATc1<sup>+</sup>CD3<sup>+</sup> cells were quantified using the Definiens Tissue Studio 4.1 software (Definiens, Munich, Germany) at the Institute of Pathology, Friedrich-Alexander-Universität Erlangen-Nürnberg (FAU), Erlangen, Germany. Whole slide images were visualized by the CaseViewer (Version 2.0, 3D Histech Ltd).

### **Total cell isolation and flow cytometry analyzes of human cells**

Frozen human tissue samples were cut into small pieces using scalpels (1–3 mm<sup>2</sup>) followed by the preparation of single-cell suspensions using the Tumor Dissociation Kit, human (Miltenyi Biotec, Bergisch Gladbach, Germany) and the gentleMACS™ Dissociator (Miltenyi Biotec) according to the manufacturer's instructions. The resulting single-cell suspension was washed and ammonium-chloride-potassium (ACK) lysis buffer was applied as previously described [27]. For flow cytometry analyzes, total cells were incubated with the respective mix of surface antibodies dissolved in PBS and incubated for 30 min at 4°C. For the intracellular staining of NFATc1 cells were fixed and permeabilized with fix/perm solution, consisting of 1% paraformaldehyde in 70% ethanol in accordance to the manufacturer's protocol (Biolegend, Fell, Germany). Antibodies used for flow cytometry are shown in Supplementary Table S1. Flow cytometric analyses were performed by using FACS Canto II (BD BioScience, Franklin Lakes, USA). Data sets were analyzed by Cell Quest Pro version 4.02 (BD BioScience,) and FlowJo v10.2 (FlowJo, LLC, Oregon, USA).

### **Cell lines**

The human A549 cell line was purchased authenticated from the ATCC bank (Manassas, Virginia, USA). ATCC authenticated cell lines by mycoplasma, bacterial and fungal contamination testing, PCR and sequencing of selected genes, human virus testing, COI assay and STR DNA profiling. We detected mycoplasma contamination using the Mycoplasma Detection Kit (Absource Diagnostics GmbH, Munich, Germany), according to the manufacturer's protocol (latest date: Aug 9, 2016). On average we perform ten cell passages between thawing and use in the described experiments. Cells were cultured in F-12K Nut mix medium (Gibco, Thermo Fisher Scientific, Langenselbold, Germany), supplemented with 10 % of fetal calf serum (FCS) (PAA Laboratories, Cölbe, Germany), 1% of the antibiotics

penicillin and streptavidin (Pen/Strep) (PAA Laboratories) and 1% of L-Glutamin (L-Glu) (Gibco, Thermo Fisher Scientific) at 37°C and 5% of CO<sub>2</sub>.

The murine LL/2-luc-M38 (LL/2) cell line was purchased and authenticated from Caliper LifeScience (Bioware cell line, Caliper LifeScience, Waltham, Massachusetts, USA). All Caliper Life Sciences cell lines are confirmed to be pathogen-free by the IMPACT profile I (PCR) at the University of Missouri Research Animal Diagnostic and Investigative Laboratory. Furthermore, the luciferase expression is coupled to a neomycin-resistance gene which renders the cell resistant to geneticin (G418). Therefore, we treated LL/2 cells with G-418 solution (500 µg/ml, Sigma-Aldrich, Taufkirchen, Germany) to select luciferase expressing cells. Three cell passages between thawing and usage in the described experiments were performed. LL/2 cells were cultured in DMEM medium (Thermo Fisher Scientific), supplemented with 10% FCS, 1% Pen/Strep and 1% L-Glu at 37°C and 5% of CO<sub>2</sub>. Mycoplasma contamination was detected using the Mycoplasma Detection Kit (Absource Diagnostics GmbH), according to the manufacturer's protocol (latest date: Aug 9, 2016).

The murine CTLL2 cell line was kindly provided to us by PD Dr. Ulrike Schleicher from the Institute of Microbiology, University Hospital Erlangen. CTLL2 were cultured in RPMI-1640 medium (Gibco, Thermo Fisher Scientific), supplemented with 10% of FCS, 1% Pen/Strep, 1% of L-Glu and 4 ng/ml IL-2 (PeproTech GmbH, Hamburg, Germany) at 37°C and 5% of CO<sub>2</sub>.

### **RNA Isolation and cDNA synthesis**

Human lung tissue samples were homogenized using Precellys Lysing Kits (Bertin Technologies, Montigny-le-Bretonneux, France) using the benchtop homogenizer Minilys (Bertin Technologies) as described in the manufacturer's protocol. Total RNA was isolated using peqGold RNA Pure (Peqlab, Erlangen, Germany) according to manufacturer's instructions. RNA was reverse-transcribed into cDNA using the RevertAid™ First Strand cDNA Synthesis Kit (Fermentas, St. Leon-Rot, Germany) in accordance to the manufacturer's instructions.

### **Quantitative Real-Time PCR (qPCR)**

qPCR of synthesized cDNA was performed by using iTaq Universal SYBR Green Supermix (BioRad, Munich, Germany) in a total volume of 20 $\mu$ l. Primers were purchased from Eurofins-MWG-Operon, Ebersberg, Germany. Primer Sequences for murine and human qPCR analyzes are depicted in Supplementary Table S2. Reactions (50 cycles, initial activation 98°C, 2min, denaturation 95°C, 5min, hybridization/elongation 60°C, 10min) were performed using the CFX-96 Real-Time PCR Detection System (BioRad), and analyzed by the CFX Manager Software (BioRad). Relative quantification was performed using the  $2^{-\Delta\Delta CT}$  method, hypoxanthine-guanine-phosphoribosyltransferase (Hprt) was used as internal standard.

### **siRNA-transfection of A549 cells and apoptosis assay**

For siRNA-mediated silencing of NFATc1,  $3 \times 10^5$  cells were incubated overnight in 6-well plates in antibiotic-free F-12K Nut mix medium containing 10 % FCS. For transfection, 25 nM NFATc1-siRNA (GE Dharmacon, Lafayette, USA) or 25 nM non-targeting control siRNA (siNT) (GE Dharmacon) were applied together with 4  $\mu$ l DharmaFECT Transfection reagent 1 (GE Dharmacon) in 2 ml antibiotic-free medium, supplemented with 10 % FCS according to the manufacturer's instructions. After 24 h incubation, transfected cells were washed with PBS and then cultured in 2 ml antibiotic-free medium, supplemented with 10 % FCS and LEAF™ Purified anti-human PD-L1 antibody (5  $\mu$ g/ml; Biolegend) or the respective LEAF™ Purified Mouse IgG2bk isotype control (5  $\mu$ g/ml; Biolegend) for 48h. For the induction of PD-L1 on A549 cells,  $3 \times 10^5$  cells were incubated o.n. +/- IFN $\gamma$  (50 ng/ml; Biolegend) followed by siRNA-mediated silencing of NFATc1 as described above and subsequent treatment with above described anti-human PD-L1 antibody or IgG2bk isotype control antibody for 24h. RNA was isolated and *NFATC1*-mRNA expression was analyzed via qPCR as described. Apoptosis assay was performed according to the manufacturer's instructions by staining the cells with Annexin V (BD Bioscience) and Propidium Iodide (BD Bioscience), followed by flow cytometry analyzes.

## **Luminescence Assay**

For luminescence analysis  $7 \times 10^3$  LL/2-luc-M38 (LL/2) cells were cultured in a 96-well plate and incubated for 24h at 37°C, 5% CO<sub>2</sub> in DMEM medium supplemented with 10% FCS, 1% Pen/Strep and 1% L-Glu. After 24h, supernatants (SN) were removed, cells were washed in PBS and incubated with either 20% lymph node-conditioned medium (LNCM) or lung-conditioned medium (LUCM). For preparation of LNCM or LUCM, total cell lysates of dLNs or lungs were cultured for 24h in the presence of  $\alpha$ CD3 (10  $\mu$ g/ml; BD Bioscience) and  $\alpha$ CD28 (1  $\mu$ g/ml; Biolegend) antibodies or in the presence of  $\alpha$ PD-1 mAb RMP1-14 (10  $\mu$ g/ml; Hölzel Diagnostika, Köln, Germany) or the respective rat IgG2a mAb 2A3 isotype control (10  $\mu$ g/ml; Hölzel Diagnostika). Resulting SN was used in LL/2 luminescence assay. After 24h incubation, LNCM or LUCM was removed and LL/2 cells were treated with 15  $\mu$ g/ml luciferin (Promega, Mannheim, Germany) to detect the luminescence intensity using the Centro XS<sup>3</sup> LB 960 Microplate Luminometer (Berthold Technologies, Bad Wildbach, Germany). Respective cell numbers were calculated by using a standard curve.

## **Apoptosis analysis of LL/2-luc-M38 cell**

For apoptosis analysis  $7 \times 10^3$  LL/2-luc-M38 (LL/2) cells were seeded in 96 well plates in DMEM medium supplemented with 10% FCS, 1% Pen/Strep and 1% L-Glu. IncuCyte™ Caspase-3/7 Reagent (Essen BioScience, Ann Arbor, Michigan, US) was used at a final concentration of 1  $\mu$ M (1:5000) and added directly to LL/2 cells in addition to 30 ng/ml rmTNF $\alpha$  (ImmunoTools, Friesoythe, Germany). Apoptotic cells (green object count, 1/mm<sup>2</sup>) were detected using the IncuCyte live-cell analysis system (Essen BioScience) over a period of 72h, images were captured every 4h. Apoptosis has been quantified as the number of green fluorescent caspase-3/7 active objects for each time point.

## **ELISA**

The enzyme-linked immunosorbent assay (ELISA) technique was utilized to analyze the cytokine concentration in cell culture supernatants. ELISA was performed in accordance with the manufacturer's instructions. Murine TNF $\alpha$ , IL-2, IL-10 and IFN $\gamma$  ELISA Sets were obtained from BD BioScience, VEGFA and IL-7 ELISA Sets from R&D Systems (Minneapolis, MN, US).

## **Mice**

NFATc1 <sup>$\Delta$ CD4</sup> and NFATc1<sup>fl/fl</sup> littermate control mice are on a C57BL/6 genetic background. These mice were together with C57BL/6 wild-type mice, kept in house at the local animal care facility of the Friedrich-Alexander-University Erlangen-Nürnberg, Hartmannstraße 14, 91052 Erlangen, under specific pathogen-free conditions. All experiments were performed in accordance with the German and European laws for animal protection and were approved by the local ethics committees of the Regierung Unterfranken (Az 55.2-2532.1-36/13).

## **Murine model of lung adenocarcinoma and *in vivo* imaging**

For tumour induction, LL/2-luc-M38 cells were cultured in DMEM medium supplemented with 10% FCS, 1% Pen/Strep and 1% L-Glu.  $1 \times 10^6$  cells suspended in 200  $\mu$ l DMEM medium (without supplements) were injected into the tail vein of 6-8 weeks old, female mice. At the indicated time points, mice were weighted and injected intraperitoneally (i.p.) with luciferin (0.15mg/g body weight; Promega). After 20 min luciferase activity was measured by the IVIS Spectrum *In Vivo* Imaging System (PerkinElmer, Waltham, USA). Luciferase activity was measured by detecting luminescence intensity (photons per second). Mice were anaesthetized with isoflurane during the measurements. Lung tumour load analysis in the lungs was performed in a logarithmic scale mode and the total flux (photons per second) was determined as previously described [29]. Blocking of PD-1 *in vivo* was performed by injecting intraperitoneally (i.p.)  $\alpha$ PD-1 mAb RMP1-14 (Hölzel Diagnostika) or the respective rat IgG2a mAb 2A3 isotype control (Hölzel Diagnostika) at 150  $\mu$ g/mouse every 4 days for maximal four injections starting at day 8

post i.v. injection of LL/2 cells. At day 20 post i.v. injection, total lung cells were isolated as previously described [30] and *in vitro* re-challenged with  $\alpha$ PD-1 mAb RMP1-14 (10  $\mu$ g/ml; Hölzel Diagnostika) or the respective rat IgG2a mAb 2A3 isotype control (10  $\mu$ g/ml; Hölzel Diagnostika) for 24h followed by flow cytometry analyses.

### **Hematoxylin and Eosin (H&E) staining on murine paraffin embedded lung sections**

Lungs were removed, fixed in 10% formalin-PBS solution, dehydrated, and embedded in paraffin. Five-micrometer-thick lung sections from paraffin blocks were stained with hematoxylin and eosin for visualization of lung tumours.

### **Flow cytometry analyzes of murine cells**

Single cell suspensions from murine lungs were prepared as previously described [30]. For total cell isolation from spleen and dLNs the same protocol was used without collagenase/DNAseI digestion. Total cells were incubated with the respective mix of surface antibodies dissolved in PBS and incubated for 30 min at 4°C. For intracellular staining cells were fixed and permeabilized with Fixation/Permeabilization concentrate/diluent in accordance to the manufacturer's protocol (eBioScience, San Diego, CA, USA). Intracellular staining of NFATc1 was performed as described above. For cytokine immunofluorescence analysis, cells were stimulated for 4 h with ionomycin (1  $\mu$ M, Sigma-Aldrich) and PMA (50 ng/mL, Sigma-Aldrich) in the presence of the Golgi inhibitor monensin (2  $\mu$ M, eBioscience). Antibodies for intracellular staining were dissolved in Permeabilization Buffer (eBioScience) and incubated 30 min at 4°C. Antibodies used for flow cytometry are shown in Supplementary Table S1. Flow cytometric analyses were performed by using FACS Calibur and FACS Canto II (BD BioScience). Data sets were analyzed by Cell Quest Pro version 4.02 (BD BioScience) and Flow-Jo v10.2 (FlowJo, LLC, Oregon, USA).

### ***In vitro* analysis of lung CD8<sup>+</sup> T-cells**

Single cell suspensions from murine lungs were prepared as previously described [30]. CD8<sup>+</sup> T-cells were isolated from the lungs of naïve and tumour-bearing mice by magnetic cell separation using the CD8a (Ly-2) MicroBeads, mouse kit (Miltenyi Biotec) in accordance to the manufacturer's instructions. The purity of the isolated CD8<sup>+</sup> T-cells was confirmed by FACS analysis. CD8<sup>+</sup> T-cells were then cultured in RPMI-1640 medium (Gibco) containing 10% FCS, 1% Pen/Strep and 1% L-Glu and stimulated with  $\alpha$ CD3 (10  $\mu$ g/ml; BD Bioscience) and  $\alpha$ CD28 (1  $\mu$ g/ml; BioLegend) antibodies. After 48h, CD8<sup>+</sup> T-cells were harvested and resuspended in 500  $\mu$ l 75% cold EtOH added dropwise. Cells were incubated for 24h at -20°C. Fixed cells were then washed twice with 1 ml wash buffer (PBS with 1% FCS, 0.09% NaN<sub>3</sub> pH 7.2) and stained with PI (BD Bioscience) staining solution (1:85 in wash buffer), followed by flow cytometric analyses by using FACS Canto II (BD BioScience).

### **Statistical analysis**

Statistics were computed with Graph-Pad Prism7. The unpaired t-test was performed for parametric data containing no more than two groups. Data are presented as mean  $\pm$  SEM and significance levels indicated as follows: \* p<0.05, \*\* p<0.01, \*\*\*p<0.001.

## Results

### Loss of *NFATC1* in the tumoural region correlates with poor prognosis in NSCLC patients

In this study we started to investigate the role of NFATc1 in NSCLC by analyzing its mRNA expression in the tumoural (TU, solid tumour), peri-tumoural (PT, 2 cm around the solid tumour) and control lung region (CTR, tumour-free control area) of our cohort of patients with lung adenocarcinoma (ADC) and lung squamous cell carcinoma (SCC), collectively grouped as NSCLC (**Table 1**). Here we found a significantly decreased expression of *NFATC1* mRNA in the TU region of patients with both ADC and SCC as compared to the respective PT and CTR region (**Fig. 1a**). Accordingly, higher amounts of total NFATc1/ $\beta$ -Actin protein levels were found in the CTR and PT region of ADC patients whereas in the TU region total NFATc1/ $\beta$ -Actin protein levels decreased (**Fig. 1b, Suppl. 1a**). In addition, we analyzed the phosphorylation status of NFATc1 (pNFATc1) as dephosphorylation of NFAT proteins leads to their activation in terms of nuclear translocation [3]. As a result, we found no differences in pNFATc1/ $\beta$ -Actin and pNFATc1/NFATc1 protein levels in the CTR, PT and TU regions (**Fig. 1b; Suppl. 1a**). We next analyzed the *NFATC1* mRNA expression in different disease stages according to the TNM classification describing the size of the primary tumour, the degree of spread to regional lymph nodes and the presence of distant metastasis. We found that, in the tumoural area, *NFATC1* mRNA expression decreased as the tumour stadium progressed (**Fig. 1c**). Moreover, using immunohistochemical double staining for NFATc1 and CD3 on lung tissue arrays obtained from our cohort of patients, we demonstrated a downregulation of NFATc1 in CD3<sup>+</sup> T-cells in the tumoural region of advanced NSCLC stages (**Fig. 1d, Suppl. 1b**). Furthermore, flow cytometry revealed an increase of NFATc1 in CD8<sup>+</sup> T-cells in the PT region as compared to the respective TU region of ADC patients (**Fig. e**), whereas in CD4<sup>+</sup> T-cells no differences of NFATc1 could be observed (**Suppl. 1c**). In addition, NFATc1 was found to be tendentially increased in CD8<sup>+</sup>PD-1<sup>+</sup> T-cells (**Fig. 1f**) in the CTR and PT region as compared to the respective TU region. No regional regulation was observed in the distribution of NFATc1 in CD4<sup>+</sup>PD-1<sup>+</sup> T-cells (**Suppl. 1d**). Regarding CD4<sup>+</sup> T-cells we observed a strong direct correlation of *NFATC1* and *CD4*

expression in the PT region (**Fig. 1g**) whereas no direct correlation was found in the\_CTR and TU region (**Suppl. 1e**). Moreover, *NFATC1* directly correlates with *TBX21* expression (**Fig. 1h**), a gene that codes for Tbet (T-box transcription factor TBX21), the main transcription factor controlling IFN $\gamma$  production in T-cells [31]. In general, these results indicate a downregulation of NFATc1 in T-cells in the presence of NSCLC and at the advanced disease stage. Furthermore, NFATc1<sup>+</sup>PD1<sup>+</sup>CD8<sup>+</sup> T-cells were found induced in the CTR and PT region of the lung of ADC patients confirming recent findings that T-cells in these patients are exhausted [32] and thus, represent the target for the  $\alpha$ PD1-tumour immunotherapy. Because NFATc1 controls the IL-2 promoter, we next correlated *NFATC1* with *IL2* and its receptor subunits IL-2R $\alpha$  (CD25), IL-2R $\beta$  (CD122) and IL-2R $\gamma$  (common cytokine receptor  $\gamma$ , CD132) [33]. We found that in the TU region *NFATC1* expression directly correlates with *IL2* as well as *CD122* and *CD132* (**Fig. 1i**) but not with *CD25* (**Suppl. 1f**). The IL-2R $\alpha$  chain is present on T effector as well as T regulatory cells. By contrast, the IL-2R $\beta$  and IL-2R $\gamma$  chain are characteristic for memory T-cells [34, 35], indicating a potential role of NFATc1 in T-cell memory expansion. In accordance to this, we found a direct correlation of *NFATC1* with the T memory cell markers *IL7* in the CTR region as well as *CD127* (IL-7R $\alpha$ ) [36] in both the CTR as well as TU region of NSCLC patients (**Fig. 1j**).

### **Influence of siRNA-mediated knockdown of NFATc1 in human lung tumour cells on the response to PD-L1 inhibitors**

Likewise PD-1 (Programmed cell death protein-1) which is highly expressed on TILs in many cancer types, its ligand PD-L1 is commonly upregulated on the tumour cell surface of different human tumours including lung cancer [37, 38]. Based on this notion, we analyzed if there is a relation between NFATc1 and PDL-1 in NSCLC development. We found a direct correlation between NFATc1 and PD-L1 in the TU region of patients suffering from NSCLC (**Fig. 2a**). Furthermore, lung cancer is of epithelial cell origin and thus, we analyzed NFATc1 in epithelial cells of the lung of these patients by using an epithelial specific antibody (anti-EpCAM). This analysis showed decreased NFATc1<sup>+</sup>PDL-1<sup>+</sup>EpCAM<sup>+</sup> cells in the TU region of ADC patients,

whereas in the CTR region, a modest proportion of EpCAM<sup>+</sup> cells expressing both NFATc1 and PD-L1 could be detected (**Fig. 2b**). We next analyzed the influence of NFATc1 on the response to PD-L1 inhibitors in lung tumour cells. To this aim we knocked down the expression of *NFATC1* in the human lung adenocarcinoma cell line A549 using *NFATC1*-directed siRNA (siNFATc1) followed by treatment with an  $\alpha$ PD-L1 antibody ( $\alpha$ PD-L1) (**Fig. 2c**). In this experimental setting, we achieved a specific *NFATC1*-knock-down as compared to non-targeting siRNA (siNT) after both  $\alpha$ PD-1 and IgG2b isotype control treatment (**Fig. 2d**). Moreover,  $\alpha$ PD-L1 antibody treatment of A549 successfully blocked PD-L1, indicated by a decreased proportion of PD-L1<sup>+</sup>PD-1<sup>-</sup> A549 cells whereas siRNA-mediated *NFATC1*-knock-down did not influence PD-L1 on A549 (**Fig. 2e, left panel**). Notably, we only detected a low proportion of PD-1<sup>+</sup>PD-L1<sup>-</sup> A549 cells (**Fig. 2e, right panel**). To get a first indication if the loss of *NFATC1* in tumour cells effects their growth, we counted A549 cells and found that *NFATC1* knock-down with or without  $\alpha$ PD-L1 antibody treatment did not affect the overall numbers of living A549 (**Fig. 2f**). Furthermore, analysis of apoptosis induction using Annexin (Ann)V/PI staining revealed a slight increase of AnnV<sup>+</sup>PI<sup>+</sup> late apoptotic A549 cells after siRNA-mediated *NFATC1*-knock-down in combination with PD-L1 blockade compared to A549 cells transfected with siNT and treated with IgG2b (**Fig. 2g**). In addition,  $\alpha$ PD-L1 antibody treatment of A549 cells in which *NFATC1* was knocked-down induced a slight expansion of AnnV<sup>+</sup>PI<sup>+</sup> dead A549 cells as compared to the IgG2b treatment (**Fig. 2g**). As we detected only a modest expression of PD-L1 by A549 cells (**Fig. 2e**), we subsequently stimulated them with IFN $\gamma$  followed by siRNA-mediated *NFATC1*-knock-down and  $\alpha$ PD-1 antibody treatment (**Fig. 2h**). IFN $\gamma$  has been shown to induce PD-L1 in human airway epithelial cells [39]. Furthermore, stimulation of A549 cells with IFN $\gamma$  mimics host immune responses as this cytokine is predominantly produced by T helper 1 (Th1) cells as well as cytotoxic CD8<sup>+</sup> T-cells to mediate successfully anti-tumoural immune responses [40]. In this experimental setting, downregulation of NFATc1 mRNA was observed by siRNA-mediated *NFATC1*-knock-down and maintained after  $\alpha$ PDL-1 antibody treatment (**Fig.2i**).While stimulation of A549 cells with IFN $\gamma$  induced a strong increase in PD-L1<sup>+</sup>PD-1<sup>-</sup> A549 cells (**Fig. 2j**), siRNA-mediated *NFATC1*-knock-

down did not influence the growth of A549 tumour cells neither in combination with  $\alpha$ PD-L1 nor with IgG2b (**Fig. 2k**). Regarding PD-1 expression, again we only detected a low proportion of PD-1<sup>+</sup>PD-L1<sup>-</sup> A549 cells (**Fig. 2j**). Altogether, NFATc1 expressed in tumour cells has no influence, neither on tumour cell growth nor on their response to  $\alpha$ PD-L1 antibody treatment.

### **Targeted deletion of NFATc1 in T-cells causes severe lung tumour development**

As we demonstrated that NFATc1 expression in tumour cells has no influence on the tumour cell growth and response to  $\alpha$ PD-L1 antibody treatment (**Fig. 2**), we started to investigate the role of NFATc1 in T-cells in a murine model of lung adenocarcinoma, a condition that closer resemble the human condition in NSCLC. Lung tumour development was induced by intravenous injection of LL/2-luc-M38 (LL/2) cells followed by the analysis of tumour growth via an *in vivo* bioluminescence based imaging system (**Fig. 3a**). Here we observed a down-regulation of NFATc1 $\alpha$  in CD4<sup>+</sup> T-cells isolated from the lung of mice suffering from lung adenocarcinoma (LL/2) as compared to those isolated from naïve control mice (naïve) (**Fig. 3b**), indicating that NFATc1 $\alpha$  mediates anti-tumoural effector functions in T-cells. Based on this observation we went on and analyzed lung adenocarcinoma development in mice with a conditional inactivation of NFATc1 in CD4<sup>+</sup> and CD8<sup>+</sup> T-cells (NFATc1 <sup>$\Delta$ CD4</sup>) compared to control littermates (NFATc1<sup>fl/fl</sup>). Here we found that, targeted deletion of NFATc1 in T-cells resulted in increased lung tumour growth as shown by bioluminescence *in vivo* imaging (**Fig. 3c**) and histological analysis indicating increased infiltration of tumour cells into the lung (**Fig. 3d**). Furthermore, we could demonstrate that *Nfatc1* was successfully deleted in T-cells of NFATc1 <sup>$\Delta$ CD4</sup> mice as shown by decreased *Nfatc1* mRNA expression in isolated lung CD8<sup>+</sup> T-cells (**Fig. 3e**) and splenic CD4<sup>+</sup> T-cells (**Fig. 3f**).

### **NFATc1 influences tissue homeostasis and differentiation of memory CD8<sup>+</sup> T-cells**

NFATc1 is highly expressed in peripheral T-cells and important for their activation and cytotoxic function [5, 7]. Thus, we next analyzed if the increased tumour growth in NFATc1 <sup>$\Delta$ CD4</sup> mice could

possibly be explained by reduced anti-tumoural T-cell-mediated immune responses. Since effector CD8<sup>+</sup> T-cells have anti-tumour functions [10, 11], we next analyzed the number of CD8<sup>+</sup> TILs in the lungs of NFATc1<sup>fl/fl</sup> and NFATc1<sup>ΔCD4</sup> mice. We found a reduced proportion CD8<sup>+</sup> T-cells in the lungs of NFATc1<sup>ΔCD4</sup> mice (**Fig. 4a**). In NFATc1<sup>ΔCD4</sup> mice bearing lung tumour, these CD8<sup>+</sup> T-cells are characterized by a decreased expression of CD25 (IL-2Rα) (**Fig. 4b**) as well as by a diminished proliferative capacity indicated by a reduced proportion of CD8<sup>+</sup> T-cells in the G2/M phase of the cell cycle (**Fig. 4c**). Furthermore, while we found no differences in the IL-2 production by lung CD8<sup>+</sup> T-cells, we could show a strong decrease in IL-2 produced by CD8<sup>+</sup> T-cells in the spleen of NFATc1<sup>ΔCD4</sup> tumour-bearing mice (**Fig. 4d**). A reduced production of IL-2 by CD8<sup>+</sup> T-cells is a characteristic feature of T-cell exhaustion [41]. Moreover, CD8<sup>+</sup> memory T-cells rely on autocrine IL-2 production which enables optimal secondary population expansion and promotes a robust response in advanced tumour-bearing states [13]. Memory CD8<sup>+</sup> T-cells are heterogeneous with respect to phenotypic markers, effector functions and tissue-homing capabilities and are classified into central memory T-cells (TCM), effector memory T-cells (TEM) and tissue-resident memory T-cells (TRM). TCM cells reside in secondary lymphoid organs and provide protection from a systemic challenge while TEM cells are highly reactive for immediate protection and circulate between lymphoid organs and peripheral tissues or inflammatory sites [15]. In the spleen of tumour-bearing NFATc1<sup>ΔCD4</sup> mice we found an increase in TCM cell populations and a trend towards reduction of TEM cells (**Fig. 4e**). Furthermore, in the tumour-bearing lung of NFATc1<sup>ΔCD4</sup> mice TEM cells were significantly decreased (**Fig. 4f**) underlining an impaired cytotoxic T-cell response in these mice. TRM cells occupy tissues and mucosal sites such as the lung and are characterized by the lack of recirculation via the bloodstream which is important for long-term regional immunity. The surface molecule integrin αE CD103 is linked to TRM cells and promotes their localization to epithelia [16]. Furthermore, NFATc1 has been shown to induce the expression of the *Itgae* gene encoding CD103 [9]. Consistently, we found a decreased proportion of CD103<sup>+</sup> TRM cells in the lung of tumour-bearing NFATc1<sup>ΔCD4</sup> mice (**Fig. 4g**) indicating an impaired tissue-homing capacity by

reduced CD103. Furthermore, in a recent study a greater density of CD103<sup>+</sup> TRM cells has been linked to an enhanced cytotoxicity of CD8<sup>+</sup> T-cells in NSCLC [42]. Thus, a reduction in CD103<sup>+</sup> TRM cell populations is accompanied by decreased cytotoxicity of CD8<sup>+</sup> T-cells, a situation which we found in the lungs of tumour-bearing NFATc1<sup>ΔCD4</sup> mice.

In general, IL-2 signals during different phases of an immune response are key in optimizing CD8<sup>+</sup> effector as well as memory T-cell functions. A loss of NFATc1 affects the production of IL-2 as well as of CD103 which influences anti-tumour effector functions of CD8<sup>+</sup> T-cells and the tissue-homing capacity of TRM cells.

### **Cytokines secreted from NFATc1<sup>ΔCD4</sup> dLNs support tumour cell growth**

Since we found a decreased expression of NFATc1 $\alpha$  in lung CD4<sup>+</sup> T-cells of tumour-bearing wild-type mice (**Fig. 3b**), we analyzed the influence of the conditional inactivation of NFATc1 in T-cells on CD4<sup>+</sup> T-cell properties in NFATc1<sup>ΔCD4</sup> mice. While we could not detect a difference in the proportion of lung CD4<sup>+</sup> T-cell populations neither in naïve nor in tumour-bearing NFATc1<sup>ΔCD4</sup> mice (**Suppl. 2a**), we found that in the absence of NFATc1, lung CD4<sup>+</sup> T-cells express a lower amount of the activation marker CD25 (IL-2R $\alpha$ ) (**Fig. 5a**). Furthermore, lung CD4<sup>+</sup> T-cells of tumour-bearing NFATc1<sup>ΔCD4</sup> mice but not of naïve mice are characterized by a reduced production of IL-2 (**Fig. 5b, Suppl. 2b**), important for T-cell proliferation, survival and activation [14]. The observed reduction of IL-2 production by lung CD4<sup>+</sup> T-cells was even more dramatically reduced by CD4<sup>+</sup> T-cells in the spleen of tumour-bearing NFATc1<sup>ΔCD4</sup> mice (**Fig. 5b**). In addition, reduced CD4<sup>+</sup> T-cell proportions in the spleen and the draining lymph nodes (dLN) of naïve and tumour-bearing NFATc1<sup>ΔCD4</sup> mice (**Fig. 5c, Suppl. 2c**) indicate an impaired CD4<sup>+</sup> T-cell development in secondary lymphoid organs. Moreover, we detected an increase of PD1 on ICOS<sup>+</sup>CD4<sup>+</sup> T-cells in the dLNs of tumour-bearing NFATc1<sup>ΔCD4</sup> mice (**Fig. 5d**). We hypothesized that the PD1<sup>+</sup>ICOS<sup>+</sup>CD4<sup>+</sup> T-cell population represents lymphocytes that are inhibited in their cytotoxic properties by T-cell exhaustion, which dampened anti-tumoural immune responses and promotes lung tumour growth. Therefore, we analyzed whether

soluble factors present in the supernatants of cells isolated from the dLNs of tumour-bearing NFATc1<sup>ΔCD4</sup> mice (=lymph node-conditioned medium, LNCM) would influence the survival of LL/2 lung tumour cells (**Fig. 5e**). We could show that, LNCM of tumour-bearing NFATc1<sup>ΔCD4</sup> mice significantly increased LL/2 cell numbers as compared to LNCM of tumour-bearing NFATc1<sup>fl/fl</sup> control littermates (**Fig. 5f**). In addition, we analyzed the influence of supernatants of total lung cells (=lung-conditioned medium, LUCM) but could not observe any effect on LL/2 cell proliferation (**Suppl. 2d, e**). Thus, LNCM but not LUCM of NFATc1<sup>ΔCD4</sup> mice contain soluble factors that promote LL/2 lung tumour cell survival. To start to identify this factor, we analyzed the presence of different cytokines and growth factors. While VEGFA, IFN $\gamma$  and IL-10 were not found to be differentially regulated (**Suppl. 2f, g, h**), we observed a decrease of TNF $\alpha$ , IL-2 and IL-7 in LNCM of NFATc1<sup>ΔCD4</sup> mice (**Fig. 5g, h, i**). Moreover, we could show that TNF $\alpha$ , an anti-tumoural cytotoxic molecule, induces apoptosis in LL/2 cells (**Fig. 5j**). In summary, during lung adenocarcinoma development, the loss of NFATc1 in CD4<sup>+</sup> T-cells resulted in decreased CD4<sup>+</sup> T-cell activation and IL-2 production in both the lung and secondary lymphoid organs. Furthermore, we could show that NFATc1 up-regulates anti-tumour cytokines in the dLNs of tumour-bearing NFATc1<sup>ΔCD4</sup> mice.

### **$\alpha$ PD-1 antibody treatment induced NFATc1 in CD4<sup>+</sup> and CD8<sup>+</sup> T-cells**

In our cohort of patients we observed an increase of NFATc1 in CD8<sup>+</sup>PD-1<sup>+</sup> T-cells in the CTR and PT region (**Fig. 1f**) confirming recent findings that T-cells in these patients are exhausted [32] probably because of chronic activation via the tumour antigen. They thus represent the target for  $\alpha$ PD-1-tumour immunotherapy. To analyze if a blockade of PD-1 influences NFATc1 in T-cells, we continued treating lung tumour-bearing B6 wild-type (WT) mice with  $\alpha$ PD-1 antibodies ( $\alpha$ PD-1) (**Fig. 6a**). In terms of survival (**Fig. 6b**) and weight change (**Fig. 6c**) we could not observe any differences between WT mice treated with  $\alpha$ PD-1 or the respective IgG2a isotype control (IgG2a). Analysis of lung tumour load revealed a trend towards reduced tumour development in  $\alpha$ PD-1-treated WT mice at day 15 post injection (p.i.) which was declined at day

18 p.i. (**Fig. 6d**). As we could not observe a difference in lung cancer development after  $\alpha$ PD-1 treatment we re-challenged total cells from the lungs of these mice with  $\alpha$ PD-1 or IgG2a *in vitro* for 24h (**Fig. 6a**). Re-challenging the lung cells *in vitro* with  $\alpha$ PD-1 antibodies induced a strong increase of NFATc1 in both CD4<sup>+</sup> and CD8<sup>+</sup> T-cells from about 70% up to 90% (**Fig. 6e, f, Suppl. 3a, b**). Afterwards, we applied supernatants of the re-challenged total lung cells (LUCM) in a cytotoxicity assay with LL/2 tumour cells used to induce lung tumour growth in mice (**Fig. 6g**). As a result we observed a reduction in LL/2 cell growth induced by LUCM of total lung cells obtained from mice bearing tumour and *in vitro* re-challenged with  $\alpha$ PD-1 as compared to IgG2a (**Fig. 6h**). Collectively these data demonstrate a strong induction of NFATc1 in T-cells by  $\alpha$ PD-1 antibody treatment which seems to inhibit LL/2 lung tumour growth via a soluble released factor. These are very supportive and challenging results in T-cells as a new therapeutic avenue for NSCLC.

## Discussion

In our present study we demonstrated an important function of NFATc1 for successful T-cell mediated anti-tumoural immune responses in the setting of NSCLC. In our human patient cohort, we found a downregulation of NFATc1 in T-cells in the presence of NSCLC and at advanced disease stages indicating that a loss of NFATc1 in T-cells is associated with poor prognosis. Upon T-cell activation, NFATc1 regulates the expression of numerous genes controlling the activity and fate of T-cells. Among them IL-2, which has been shown to be important for T-cell activation, proliferation and survival as well as for CD8<sup>+</sup> effector and memory T-cell generation [9, 14, 17]. Accordingly, we found a direct correlation between NFATc1 and IL-2 as well as its receptor subunits CD122 and CD132 but not CD25. While immunosuppressive T regulatory cells are characterized by the expression of all three IL2-R subunits, CD122 and CD132 are characteristic for memory T-cells and NK cells [34, 35]. Among fate markers for memory T-cells, the *IL7R* genes are NFATc1 targets[9]. According to that, NFATc1 correlates with the IL7R $\alpha$  chain as well as with IL-7 implicated in CD8<sup>+</sup> memory T-cell differentiation and homeostasis [9, 36]. In addition, NFATc1 directly correlates with Tbet, the main transcription factor controlling IFN $\gamma$  that is relevant for the cytotoxic anti-tumour activity of TIL [31], which was found downregulated in the CD8<sup>+</sup> T-cells isolated from the tumoural region of our cohort of patients with NSCLC [27]. Thus, in the tumoural and control region of NSCLC patients, NFATc1 correlates with factors that are characteristic for cytotoxic and memory T-cell responses and seems to be important for anti-tumoural immunity.

In our murine model of lung adenocarcinoma we found a decreased expression of NFATc1 $\alpha$  in lung CD4<sup>+</sup> T-cells of tumour-bearing wild-type mice. Moreover, targeted deletion of NFATc1 in T-cells (NFATc1<sup>ACD4</sup>) resulted in increased lung tumour growth which was associated with an impairment of CD4<sup>+</sup> and CD8<sup>+</sup> T-cells consistent with the importance of NFATc1 for T-cell activation and cytotoxic T-cell functions [5, 7]. We further detected reduced CD8<sup>+</sup> T-cell proportions as well as decreased proliferation of CD8<sup>+</sup> T-cells in the tumour-bearing lung of

NFATc1<sup>ΔCD4</sup> mice. The production of IL-2 by lung CD8<sup>+</sup> T-cells was not influenced while splenic CD8<sup>+</sup> T-cells were characterized by a strongly decreased IL-2 secretion. IL-2 contributes to the primary as well as secondary expansion of CD8<sup>+</sup> T-cells. Since the magnitude of T-cell expansion defines the number of memory CD8<sup>+</sup> T-cells, IL-2 influences memory cell generation. Furthermore, at the memory state, CD8<sup>+</sup> T-cell frequencies can be strengthened by administration of IL-2 [13, 17]. Consistently, we found a reduction of TEM cell populations in the spleen and the lung of tumour-bearing NFATc1<sup>ΔCD4</sup> mice underlining an impaired cytotoxic T-cell response in these mice. Interestingly, splenic TCM cells of tumour-bearing NFATc1<sup>ΔCD4</sup> mice were significantly increased. The capacity to secrete IL-2 has been associated with TCM cells rather than TEM cells [15]. Thus, even though we detected an increased TCM cell population in the spleen of tumour-bearing NFATc1<sup>ΔCD4</sup> mice, we suggest that these cells are ineffective in secreting IL-2 as indicated by a reduced IL-2 production by splenic CD8<sup>+</sup> T-cells. This reduced IL-2 production could inhibit the development of splenic TEM cells as IL-2 signals are able to rescue CD8<sup>+</sup> T-cells from cell death and provide an increase in CD8<sup>+</sup> memory T-cell counts [17]. Furthermore, as TEM cells circulate between lymphoid organs and peripheral tissue a decreased splenic TEM cell population is accompanied by a reduction in lung TEM cells in tumour-bearing NFATc1<sup>ΔCD4</sup>. A recent study described increased TCM and decreased TEM cell populations in the spleen of *Listeria monocytogenes* infected NFATc1<sup>ΔCD4</sup> [9] which is similar to the results we obtained in the murine lung adenocarcinoma model. Beside TEM and TCM cell populations we also analyzed the proportion of TRM cells, a unique tissue-resident memory T-cell subset important for enhanced regional immunity. TRM cells in various non-lymphoid tissues are characterized by the integrin αE CD103 which promotes the localization to epithelia [16]. In the tumour-bearing lung of NFATc1<sup>ΔCD4</sup> mice we found a strong decrease of CD103<sup>+</sup> TRM cells consistent with the finding that NFATc1 has been shown to induce the expression of the *Itgae* gene encoding CD103 [9]. These results indicate that the tissue-homing capacity of lung TRM cells of tumour-bearing NFATc1<sup>ΔCD4</sup> mice is impaired. In addition, in a recent study a greater density of CD103<sup>+</sup> TRM cells has been linked to an enhanced cytotoxicity of CD8<sup>+</sup> T-cells and

was predictive for a better survival outcome of lung cancer patients [42]. Thus, a reduction in CD103<sup>+</sup> TRM cell populations is accompanied by a decreased function and cytotoxicity of CD8<sup>+</sup> T-cells, a situation which we found in the lungs of tumour-bearing NFATc1<sup>ΔCD4</sup> mice mainly promoted by decreased IL-2.

Furthermore, we found decreased CD4<sup>+</sup> T-cell proportions that produced reduced amounts of IL-2 in secondary lymphoid organs of tumour-bearing NFATc1<sup>ΔCD4</sup> mice indicating impaired T-cell activation and effector functions also in terms of CD4<sup>+</sup> T-cells. Interestingly, in the dLN of tumour-bearing NFATc1<sup>ΔCD4</sup> mice we found a strongly increased proportion of PD-1 on ICOS<sup>+</sup>CD4<sup>+</sup> T-cells. High expression of PD-1 is a key feature of T-cell exhaustion, a state of T-cell dysfunction defined by inhibited cytotoxic properties [18, 41]. Furthermore, ICOS has been described to be crucial for the expansion and suppressive activity of Foxp3<sup>+</sup> T regulatory cells as well as for IL-10 production [43]. Thus, we hypothesized that the PD1<sup>+</sup>ICOS<sup>+</sup>CD4<sup>+</sup> T-cell population represents highly suppressive lymphocytes affecting T-cell effector functions and inhibiting anti-tumoural immune responses while promoting tumour growth. This was supported by the fact that lymph node-conditioned medium (LNCM) of tumour-bearing NFATc1<sup>ΔCD4</sup> mice induced LL/2 tumour cell survival. Consistently, we found a decreased production of TNFα. TNFα is a pleiotropic cytokine with pro- and anti-tumoural functions as it regulates diverse events like proliferation, invasion and apoptosis [44]. We could show that TNFα induced apoptosis in LL/2 lung tumour cells, underlining its ability to suppress tumour cell proliferation and induce tumour regression in our murine model of lung adenocarcinoma. Moreover, reduced proportion of IL-7 in LNCM confirms impaired memory T-cell responses in the absence of NFATc1.

Immune checkpoint blockade with αPD-1 or αPD-L1 has proven to be a highly promising treatment of human cancers, including lung cancer [19, 22, 23]. As lung cancer is of epithelial cell origin and NFATc1 has been described to be expressed in mouse lung epithelial cells, [45] we analyzed if there is a correlation of NFATc1 and PD-L1 in EpCAM<sup>+</sup> epithelial cells in the different regions of NSCLC patients. We found a direct correlation between NFATc1 and PDL-1 in the TU region of NSCLC patients, whereas NFATc1<sup>+</sup>PDL-1<sup>+</sup>EpCAM<sup>+</sup> cells decreased

indicating that epithelial cells expressing NFATc1 together with PD-L1 are not present in the TU region of the lung. Furthermore, using *NFATC1*-directed siRNA followed by  $\alpha$ PD-L1 antibody treatment of the human lung adenocarcinoma cell line A549, we could show that, NFATc1 expressed in tumour cells has no influence on tumour cell growth and their response to  $\alpha$ PD-L1 antibody treatment. After this observation we focused on NFATc1 and PD-1 expression in T-cells in the setting of NSCLC. We found that NFATc1 is induced in CD8<sup>+</sup>PD-1<sup>+</sup>-T-cells of the CTR and PT region of the lung of ADC patients. In the tumour microenvironment, tumour antigens induce a durative activation of T-cells which probably contributes to T-cell exhaustion via PD-1 and promotes the impairment of effector functions [41, 46]. As NFATc1 is important for T-cell activation [3, 9] and has been shown to induce the expression of PD-1, [24] the NFATc1<sup>+</sup>PD-1<sup>+</sup>CD8<sup>+</sup>-T-cells could represent exhausted T-cells that are targets for  $\alpha$ PD1-tumour immunotherapy. Indeed, we could show that re-challenged total lung cells of tumour-bearing wild-type mice with  $\alpha$ PD-1 antibodies induced a strong increase of NFATc1 from about 70% up to 90% in T-cells. This strong increase could be explained by the PD-1 signaling pathway: triggering of PD-1 by its ligand PD-L1 expressed on tumour cells induces the inhibition of the phosphatidylinositol-3-kinase (PI3K)/Akt pathway. Akt normally negatively regulates the glycogen-synthase kinase 3 (GSK3) which inhibits NFATc1 [3, 25, 26]. Thus, the blockade of PD-1 restores TCR signaling, ensured the activation of Akt which inhibits GSK3 and promotes the activation of NFATc1 which induces T-cell activation and effector functions [7, 9, 25]. Although preliminary, this is a very promising avenue: to challenge T-cells of patients with  $\alpha$ -PD1 antibodies *ex vivo* to induce NFATc1 and promote T-cell activation followed by the transfer of these cells back into the patients to boost anti-tumoural T-cell responses. In fact, supernatants of lung cells re-challenged with  $\alpha$ -PD1 antibodies inhibited LL/2 lung tumour cell growth supporting the importance of NFATc1 for T-cell mediated cytotoxic immune responses.

## **Acknowledgments**

This work was supported by the SFB643 (Project B12) in Erlangen and by the Department of Molecular Pneumology. We thank the whole team at the Department of Molecular Pneumology, especially Sonja Trump, Susanne Mittler and Adriana Geiger for their technical help, as well as the team at the Department of Thoracic Surgery and the Institute of Pathology at the University Hospital, Friedrich-Alexander-Universität Erlangen-Nürnberg, for their help and support to this work. Furthermore, we thank Dr. Paolo Ceppi at the Interdisciplinary Center for Clinical Research at the Friedrich-Alexander-Universität Erlangen-Nürnberg, for giving us the opportunity to perform apoptosis analysis using the IncuCyte live-cell analysis system.

## References

1. Crabtree, G. and E. Olson, *NFAT Signaling: Choreographing Review the Social Lives of Cells*. *Cell* 109. S67–S79, 2002.
2. Hogan, P.G., et al., *Transcriptional regulation by calcium, calcineurin, and NFAT*. *Genes & development*, 2003. **17**(18): p. 2205-2232.
3. Macian, F., *NFAT proteins: key regulators of T-cell development and function*. *Nature reviews. Immunology*, 2005. **5**(6): p. 472.
4. Rumi-Masante, J., et al., *Structural basis for activation of calcineurin by calmodulin*. *Journal of molecular biology*, 2012. **415**(2): p. 307-317.
5. Serfling, E., et al., *NFATc1 autoregulation: a crucial step for cell-fate determination*. *Trends in immunology*, 2006. **27**(10): p. 461-469.
6. Chuvpilo, S., et al., *Multiple NF-ATc isoforms with individual transcriptional properties are synthesized in T lymphocytes*. *The Journal of Immunology*, 1999. **162**(12): p. 7294-7301.
7. Chuvpilo, S., et al., *Autoregulation of NFATc1/A expression facilitates effector T cells to escape from rapid apoptosis*. *Immunity*, 2002. **16**(6): p. 881-895.
8. Serfling, E., et al., *NFATc1/αA: the other face of NFAT factors in lymphocytes*. *Cell Communication and Signaling*, 2012. **10**(1): p. 16.
9. Klein-Hessling, S., et al., *NFATc1 controls the cytotoxicity of CD8+ T cells*. *Nature Communications*, 2017. **8**(1): p. 511.
10. Schwarz, E.C., B. Qu, and M. Hoth, *Calcium, cancer and killing: the role of calcium in killing cancer cells by cytotoxic T lymphocytes and natural killer cells*. *Biochimica et Biophysica Acta (BBA)-Molecular Cell Research*, 2013. **1833**(7): p. 1603-1611.
11. Hadrup, S., M. Donia, and P. thor Straten, *Effector CD4 and CD8 T cells and their role in the tumor microenvironment*. *Cancer Microenvironment*, 2013. **6**(2): p. 123-133.
12. Rooney, J.W., et al., *Novel NFAT sites that mediate activation of the interleukin-2 promoter in response to T-cell receptor stimulation*. *Molecular and Cellular Biology*, 1995. **15**(11): p. 6299-6310.
13. Feau, S., et al., *Autocrine IL-2 is required for secondary population expansion of CD8+ memory T cells*. *Nature immunology*, 2011. **12**(9): p. 908-913.
14. Boyman, O. and J. Sprent, *The role of interleukin-2 during homeostasis and activation of the immune system*. *Nature reviews. Immunology*, 2012. **12**(3): p. 180.
15. Klebanoff, C.A., L. Gattinoni, and N.P. Restifo, *CD8+ T-cell memory in tumor immunology and immunotherapy*. *Immunological reviews*, 2006. **211**(1): p. 214-224.
16. Mueller, S.N. and L.K. Mackay, *Tissue-resident memory T cells: local specialists in immune defence*. *Nature reviews Immunology*, 2016. **16**(2): p. 79.
17. Boyman, O., J.-H. Cho, and J. Sprent, *The role of interleukin-2 in memory CD8 cell differentiation*, in *Memory T Cells*. 2010, Springer. p. 28-41.
18. Wherry, E.J., *T cell exhaustion*. *Nature immunology*, 2011. **12**(6): p. 492-499.
19. Baitsch, L., et al., *The three main stumbling blocks for anticancer T cells*. *Trends in immunology*, 2012. **33**(7): p. 364-372.
20. Wolchok, J.D., et al., *Nivolumab plus ipilimumab in advanced melanoma*. *New England Journal of Medicine*, 2013. **369**(2): p. 122-133.
21. Sharma, P. and J.P. Allison, *Immune checkpoint targeting in cancer therapy: toward combination strategies with curative potential*. *Cell*, 2015. **161**(2): p. 205-214.
22. Sundar, R., et al., *Nivolumab in NSCLC: latest evidence and clinical potential*. *Therapeutic advances in medical oncology*, 2015. **7**(2): p. 85-96.

23. Baumeister, S.H., et al., *Coinhibitory pathways in immunotherapy for cancer*. Annual review of immunology, 2016. **34**: p. 539-573.
24. Oestreich, K.J., et al., *NFATc1 regulates PD-1 expression upon T cell activation*. The Journal of Immunology, 2008. **181**(7): p. 4832-4839.
25. Sakuishi, K. and A.C. Anderson, *Tim-3 Regulation of Cancer Immunity*, in *Tumor-Induced Immune Suppression*. 2014, Springer. p. 239-261.
26. Boussiotis, V.A., P. Chatterjee, and L. Li, *Biochemical signaling of PD-1 on T cells and its functional implications*. Cancer journal (Sudbury, Mass.), 2014. **20**(4): p. 265.
27. Andreev, K., et al., *Impaired T-bet-pSTAT1 $\alpha$  and perforin-mediated immune responses in the tumoral region of lung adenocarcinoma*. British journal of cancer, 2016. **115**(9): p. e11.
28. Eisenhut, F., et al., *FAM13A is associated with non-small cell lung cancer (NSCLC) progression and controls tumor cell proliferation and survival*. Oncoimmunology, 2017. **6**(1): p. e1256526.
29. Reppert, S., et al., *A role for T-bet-mediated tumour immune surveillance in anti-IL-17A treatment of lung cancer*. Nature communications, 2011. **2**: p. 600.
30. Sauer, K.A., et al., *Isolation of CD4 $^{+}$  T cells from murine lungs: a method to analyze ongoing immune responses in the lung*. Nature protocols, 2006. **1**(6): p. 2870-2875.
31. Lazarevic, V., L.H. Glimcher, and G.M. Lord, *T-bet: a bridge between innate and adaptive immunity*. Nature Reviews Immunology, 2013. **13**(11): p. 777-789.
32. Vahl, J.M., et al., *Interleukin-10-regulated tumour tolerance in non-small cell lung cancer*. British journal of cancer, 2017. **117**(11): p. 1644.
33. Malek, T.R., *The biology of interleukin-2*. Annu. Rev. Immunol., 2008. **26**: p. 453-479.
34. Surh, C.D. and J. Sprent, *Homeostasis of naive and memory T cells*. Immunity, 2008. **29**(6): p. 848-862.
35. Shevach, E.M., *Application of IL-2 therapy to target T regulatory cell function*. Trends in immunology, 2012. **33**(12): p. 626-632.
36. Huster, K.M., et al., *Selective expression of IL-7 receptor on memory T cells identifies early CD40L-dependent generation of distinct CD8 $^{+}$  memory T cell subsets*. Proceedings of the National Academy of Sciences of the United States of America, 2004. **101**(15): p. 5610-5615.
37. Konishi, J., et al., *B7-H1 expression on non-small cell lung cancer cells and its relationship with tumor-infiltrating lymphocytes and their PD-1 expression*. Clinical cancer research, 2004. **10**(15): p. 5094-5100.
38. Pardoll, D.M., *The blockade of immune checkpoints in cancer immunotherapy*. Nature Reviews Cancer, 2012. **12**(4): p. 252.
39. Kim, J., et al., *Constitutive and inducible expression of b7 family of ligands by human airway epithelial cells*. American journal of respiratory cell and molecular biology, 2005. **33**(3): p. 280-289.
40. Ikeda, H., L.J. Old, and R.D. Schreiber, *The roles of IFN $\gamma$  in protection against tumor development and cancer immunoediting*. Cytokine & growth factor reviews, 2002. **13**(2): p. 95-109.
41. Pauken, K.E. and E.J. Wherry, *Overcoming T cell exhaustion in infection and cancer*. Trends in immunology, 2015. **36**(4): p. 265-276.
42. Ganesan, A.-P., et al., *Tissue-resident memory features are linked to the magnitude of cytotoxic T cell responses in human lung cancer*. Nature immunology, 2017. **18**(8): p. 940.
43. Redpath, S.A., et al., *ICOS controls Foxp3 $^{+}$  regulatory T-cell expansion, maintenance and IL-10 production during helminth infection*. European journal of immunology, 2013. **43**(3): p. 705-715.

44. Wang, X. and Y. Lin, *Tumor necrosis factor and cancer, buddies or foes?* Acta Pharmacologica Sinica, 2008. **29**(11): p. 1275-1288.
45. Davé, V., T. Childs, and J.A. Whitsett, *Nuclear factor of activated T cells regulates transcription of the surfactant protein D gene (Sftpd) via direct interaction with thyroid transcription factor-1 in lung epithelial cells.* Journal of Biological Chemistry, 2004. **279**(33): p. 34578-34588.
46. Jiang, Y., Y. Li, and B. Zhu, *T-cell exhaustion in the tumor microenvironment.* Cell death & disease, 2015. **6**(6): p. e1792.

**Table 1. Clinical data of the NSCLC patient cohort analysed in this study.**

Sample number	Sample ID	Histological Classification	Maximal tumour diameter (cm)	T	N	M	TNM Stadium	Gender	Age	Average Smoking (P/Y)
1	1-MP	SCC	1,3	1b	0	0	IA	Male	80	40
2	2-MP	SCC	5,1	1a	0	0	IA	Male	57	40
3	3-MP	ADC	5	2a	0	0	IB	Male	79	60
4	4-MP	SCC	2	1b	1	0	IIA	Female	53	25
5	8-MP	SCC	5,5	3	0	0	IBB	Male	66	30
6	9-MP	ADC	2,7	1b	2	0	IIIA	Female	84	0
7	13-MP	SCC	3	1b	0	0	IA	Male	69	50
8	14-MP	SCC	1,9	1a	0	0	IA	Female	58	30
9	15-MP	ADC	2,5	1b	0	0	IA	Male	63	100
10	16-MP	ADC	4,6	3	0	0	IBB	Female	70	15
11	17-MP	ADC	2,6	2	0	0	IB	Male	74	70
12	19-MP	ADC	6,5	2b	0	0	IIA	Female	55	30
13	20-MP	ADC	2,8	1b	0	0	IA	Male	65	60
14	21-MP	SCC	2,5	1b	0	0	IA	Male	41	10
15	22-MP	ADC	7	2b	1	0	IBB	Male	68	82
16	23-MP	ADC	4,5	2a	0	0	IB	Male	73	75
17	26-MP	ADC	1,3	1a	0	1	IV	Female	52	50
18	27-MP	ADC	1,4	1a	0	0	IA	Female	70	50
19	28-MP	ADC	1,2	1a	0	0	IA	Male	76	60
20	29-MP	SCC	3,7	1b	0	0	IBB	Male	74	100
21	30-MP	SCC	1,8	1a	0	0	IA	Female	70	30
22	32-MP	ADC	4,4	2a	2	0	IIIA	Female	60	30
23	34-MP	ADC	1,8	1	0	0	IA	Female	51	45
24	35-MP	ADC	3	1b	0	0	IA	Female	72	0
25	36-MP	SCC	3,5	2a	1	0	IB	Male	74	40
26	37-MP	SCC	3,3	2a	1	0	IIA	Male	60	45
27	40-MP	ADC	1,8	1a	1	0	IIA	Male	82	100
28	41-MP	SCC	1,3	3	1	0	IIIA	Male	70	42
29	42-MP	SCC	1,5	2b	1	0	IBB	Male	74	40
30	43-MP	ADC	4	2a	2	0	IIIA	Female	72	0
31	44-MP	ADC	1,5	1a	0	0	IA	Male	53	70
32	46-MP	SCC	9,5	3	1	0	IIIA	Male	60	30
33	47-MP	SCC	6	2b	0	0	IIA	Male	64	80
34	48-MP	SCC	5	2b	0	0	IIA	Male	55	20
35	50-MP	SCC	2,5	3	1	0	IIIA	Male	70	0
36	51-MP	ADC	2,4	1b	2	1	IV	Male	62	90
37	52-MP	ADC	#	#	#	#	#	#	#	#
38	53-MP	ADC	2,25	1a	0	0	IA	Male	62	10
39	54-MP	SCC	4,1	3	0	0	IBB	Male	72	0
40	55-MP	ADC	1,8	1a	2	0	IIIA	Female	64	40
41	56-MP	ADC	4	2a	0	0	IB	Female	67	0
42	57-MP	ADC	3,8	2a	0	0	IB	Female	35	10
43	58-MP	ADC	6,5	3	0	0	IBB	Female	69	0
44	59-MP	ADC	0,9	4	0	0	IIIA	Male	70	#
45	60-MP	SCC	2,5	1b	1	0	IIA	Male	71	#
46	61-MP	SCC	1,1	1a	0	0	IA	Male	75	#
47	62-MP	ADC	3,5	1b	0	0	IA	Female	80	#
48	63-MP	SCC	9	3	1	0	IIIA	Male	69	#
49	64-MP	ADC	3,5	1b	0	0	IA	Male	55	35
50	65-MP	SCC	2,8	1b	0	0	IA	Female	76	#
51	68-MP	ADC	8	3	0	0	IBB	Male	42	22
52	69-MP	ADC	#	#	#	#	#	#	#	#
53	73-MP	ADC	4,8	2a	0	0	IB	Female	67	22
54	74-MP	ADC	3,2	2a	0	0	IB	Female	58	#
55	75-MP	SCC	4,8	2a	1	0	IIA	Male	54	35
56	105-MP	ADC	1,8	1a	0	0	IA	Male	77	35
57	106-MP	ADC	1,2	1a	0	0	IA	Male	79	60
58	108-MP	ADC	3,6	2a	0	0	IB	Female	60	40

**T-primary tumour:** 0: No evidence of primary tumour; 1a: Tumour 2 cm or less in greatest dimension; 1b: Tumour more than 2 cm but not more than 3 cm in greatest dimension; 2a: Tumour more than 3 cm but not more than 5 cm in greatest dimension; 2b: Tumour more than 5 cm but not more than 7 cm in greatest dimension; 3: Tumour more than 7 cm;

**N-regional lymph nodes:** 0: No regional lymph node metastasis; 1: Metastasis in ipsilateral peribronchial and/ or ipsilateral hilar lymph nodes and intrapulmonary nodes, including involvement by direct extension; 2: Metastasis in ipsilateral mediastinal and/or subcarinal lymph node(s);

**M-distant metastasis:** 0: No distant metastasis; 1: Distant metastasis;

**Histopathological grading:** G1: well differentiated; G2: moderately differentiated; G3: Poorly differentiated; # No information available

## Figure legends

### Figure 1: Loss of *NFATC1* correlates with poor prognosis of NSCLC patients.

**a**, qPCR based analysis of *NFATC1* mRNA expression in lung tissue samples from the tumoural (TU), peritumoural (PT) and control (CTR) region of patients suffering from adenocarcinoma (ADC:  $N_{CTR}=30$ ,  $N_{PT}=25$ ,  $N_{TU}=26$ ) or squamous cell carcinoma (SCC:  $N_{CTR}=17$ ,  $N_{PT}=18$ ,  $N_{TU}=18$ ) collectively grouped as non-small cell lung cancer (NSCLC:  $N_{CTR}=47$ ,  $N_{PT}=43$ ,  $N_{TU}=44$ ). **b**, Quantitative Western Blot analysis of total NFATc1/ $\beta$ -Actin, pNFATc1/ $\beta$ -Actin and pNFATc1/NFATc1 protein levels in the CTR, PT and TU area of patients with ADC ( $N_{CTR}=6$ ,  $N_{PT}=6$ ,  $N_{TU}=5$ ). **c**, Expression analysis of *NFATC1* mRNA in the TU region of ADC patients (IA:  $N_{TU}=7$ ; IIA:  $N_{TU}=2$ ; IIIA:  $N_{TU}=4$ ), SCC patients (IA:  $N_{TU}=5$ ; IIA:  $N_{TU}=5$ ; IIIA:  $N_{TU}=4$ ) and total NSCLC patients (IA:  $N_{TU}=12$ ; IIA:  $N_{TU}=7$ ; IIIA:  $N_{TU}=8$ ) classified according to the TNM staging system. **d**, Double immunohistochemistry (IHC) for NFATc1 (brown) and CD3 (blue) on lung tissue array in the TU region of NSCLC patients classified according to the TNM staging system (IA:  $N_{TU}=7$ ; IIA:  $N_{TU}=2$ ; IIIA:  $N_{TU}=1$ , 60x magnification). **e-f**, Flow cytometry analyses of NFATc1 in CD8<sup>+</sup> T-cells (%) **e**, and NFATc1 in PD-1<sup>+</sup>CD8<sup>+</sup> T-cells (%) **f**, in total lung cell suspension of the CTR, PT and TU region from ADC patients (ADC:  $N_{CTR}=3$ ,  $N_{PT}=3$ ,  $N_{TU}=3$ ). **g-h**, Correlation between lung *NFATC1* and: *CD4* ( $N_{PT}=41$ ) expression in the PT region **g**, *TBX21* ( $N_{TU}=38$ ) expression in the TU region **h**, *IL2* ( $N_{TU}=23$ ), *CD122* ( $N_{TU}=36$ ) and *CD132* ( $N_{TU}=35$ ) expression in the TU region **i**, *IL7* ( $N_{CTR}=37$ ), *CD127* ( $N_{CTR}=41$ ) expression in the CTR region and *CD127* ( $N_{TU}=40$ ) expression in the TU region **j**, from patients with NSCLC. N values are given per group. Data are shown as mean values  $\pm$  s.e.m. using student's two-tailed t-test \*P,0.05; \*\*P,0.01, \*\*\*P,0.001.

**Figure 2: Influence of siRNA-mediated knockdown of NFATc1 in tumour cells on the response to PD-L1 inhibitors.**

**a**, Correlation between *NFATC1* and *PD-L1* ( $N_{TU}=24$ ) mRNA expression in the lung TU region of patients with NSCLC. **b**, Flow cytometry analysis of  $NFATc1^+PD-L1^+EpCAM^+$  cells (%) in total lung cell suspension of the CTR, PT and TU region of ADC patients ( $N_{CTR}=3$ ,  $N_{PT}=3$ ,  $N_{TU}=3$ ). **c**, Experimental design: A549 cells were cultured overnight (o.n.) followed by transfection with a *NFATC1*-directed siRNA (siNFATc1) or a non-targeting siRNA (siNT). Twenty-four h later, A549 cells were incubated with 5  $\mu$ g/ml  $\alpha$ PD-L1 antibody or IgG2b isotype control followed by another 48h incubation time and subsequently analysis of **d**, *NFATC1* mRNA expression **e**,  $PD-L1^+PD-1^-$  as well as  $PD-L1^-PD-1^+$  A549 cells (%), **f**, A549 cell number and **g**,  $AnnV^+PI^+$  and  $AnnV^-PI^+$  apoptotic A549 cells (IgG2b:  $N_{siNT}=6$ ,  $N_{siNFATc1}=6$ ;  $\alpha$ PD-L1:  $N_{siNT}=6$ ,  $N_{siNFATc1}=6$ ). **h**, Experimental design: A549 cells were cultured with +/- 50 ng/ml  $IFN\gamma$  for 24h followed by transfection with siNFATc1 or siNT. 24h later A549 cells were incubated with 5  $\mu$ g/ml  $\alpha$ PD-L1 antibody or IgG2b isotype control followed by another 24h incubation time and subsequently analysis of **i**, *NFATC1* mRNA expression **j**,  $PD-L1^+PD-1^-$  as well as  $PD-L1^-PD-1^+$  A549 cells (%) and **k**, A549 cell number (Unstimulated US:  $N_{siNT}=3$ ,  $N_{siNFATc1}=3$ ;  $IFN\gamma$ :  $N_{siNT}=3$ ,  $N_{siNFATc1}=3$ ;  $IFN\gamma+IgG2b$ :  $N_{siNT}=3$ ,  $N_{siNFATc1}=3$ ;  $IFN\gamma+\alpha$ PD-L1:  $N_{siNT}=3$ ,  $N_{siNFATc1}=3$ ). N values are given per group. Data are shown as mean values  $\pm$  s.e.m. using student's two-tailed t-test \*P,0.05; \*\*P,0.01, \*\*\*P,0.001.

**Figure 3: Targeted deletion of NFATc1 in T-cells causes severe lung tumour development.**

**a**, Experimental design for the induction of lung adenocarcinoma development in mice. Tumour growth was induced via intravenous (i.v.) injection of LL/2-luc-M38 (LL/2) lung carcinoma cells. Tumour load was measured using an *in vivo* bioluminescence based imaging system. The experiment ended on day 16 to 21. **b**, qPCR based analysis of *Nfatc1alpha* mRNA expression in isolated lung  $CD4^+$  T-cells of naïve and tumour-bearing wild type mice (LL/2) ( $N_{naïve}=5$ ,  $N_{LL/2}=5$ ). **c**, Representative *in vivo* images of lung tumour load analysis in  $NFATc1^{fl/fl}$  control littermates ( $NFATc1^{fl/fl}+LL/2$ ) and  $NFATc1^{\Delta CD4}$  ( $NFATc1^{\Delta CD4}+LL/2$ ) mice (left). Radiance (photone flux/second) of the last day of three independent experiments was summarized (right),

( $N_{\text{NFATc1}^{\text{fl/fl}}+\text{LL}/2} = 13$ ,  $N_{\text{NFATc1}\Delta\text{CD4}+\text{LL}/2} = 14$ ). **d**, Representative H&E staining of the lung of a  $\text{NFATc1}^{\text{fl/fl}}$  and  $\text{NFATc1}^{\Delta\text{CD4}}$  mouse. **e**, qPCR based analysis of *Nfatc1* mRNA expression in isolated lung  $\text{CD8}^+$  T-cells of tumour-bearing  $\text{NFATc1}^{\text{fl/fl}}$  and  $\text{NFATc1}^{\Delta\text{CD4}}$  mice ( $N_{\text{NFATc1}^{\text{fl/fl}}+\text{LL}/2} = 4$ ,  $N_{\text{NFATc1}\Delta\text{CD4}+\text{LL}/2} = 3$ ). **f**, qPCR based analysis of *Nfatc1* mRNA expression in isolated  $\text{CD4}^+$  T-cells from the spleen of lung tumour-bearing  $\text{NFATc1}^{\text{fl/fl}}$  and  $\text{NFATc1}^{\Delta\text{CD4}}$  mice ( $N_{\text{NFATc1}^{\text{fl/fl}}+\text{LL}/2} = 3$ ,  $N_{\text{NFATc1}\Delta\text{CD4}+\text{LL}/2} = 2$ ). N values are given per group. Data are shown as mean values  $\pm$  s.e.m. using student's two-tailed t-test \*P,0.05; \*\*P,0.01, \*\*\*P,0.001.

**Figure 4: NFATc1 influences tissue homeostasis and differentiation of memory  $\text{CD8}^+$  T-cells.**

**a**, Flow cytometry analyses of  $\text{CD8}^+$  T-cells (%) in total lung cell suspension of naive and lung tumour-bearing  $\text{NFATc1}^{\text{fl/fl}}$  and  $\text{NFATc1}^{\Delta\text{CD4}}$  mice ( $N_{\text{NFATc1}^{\text{fl/fl}}} = 12$ ,  $N_{\text{NFATc1}\Delta\text{CD4}} = 11$ ;  $N_{\text{NFATc1}^{\text{fl/fl}}+\text{LL}/2} = 11$ ,  $N_{\text{NFATc1}\Delta\text{CD4}+\text{LL}/2} = 13$ ). **b**, Flow cytometry analyses of  $\text{CD25}^+$  expressing  $\text{CD8}^+$  T-cells (%) in total lung cell suspension of lung tumour-bearing  $\text{NFATc1}^{\text{fl/fl}}$  and  $\text{NFATc1}^{\Delta\text{CD4}}$  mice ( $N_{\text{NFATc1}^{\text{fl/fl}}+\text{LL}/2} = 8$ ,  $N_{\text{NFATc1}\Delta\text{CD4}+\text{LL}/2} = 11$ ). **c**, PI proliferation analysis of  $\text{CD8}^+$  T-cells isolated from the lungs of naive and tumour-bearing  $\text{NFATc1}^{\text{fl/fl}}$  and  $\text{NFATc1}^{\Delta\text{CD4}}$  mice ( $N_{\text{NFATc1}^{\text{fl/fl}}} = 3$ ,  $N_{\text{NFATc1}\Delta\text{CD4}} = 3$ ;  $N_{\text{NFATc1}^{\text{fl/fl}}+\text{LL}/2} = 4$ ,  $N_{\text{NFATc1}\Delta\text{CD4}+\text{LL}/2} = 4$ ). **d**, Flow cytometry analysis of IL-2 production by  $\text{CD8}^+$  T-cells (%) in total cell suspension of the lung and the spleen of tumour-bearing  $\text{NFATc1}^{\text{fl/fl}}$  and  $\text{NFATc1}^{\Delta\text{CD4}}$  mice (Lung:  $N_{\text{NFATc1}^{\text{fl/fl}}+\text{LL}/2} = 8$ ,  $N_{\text{NFATc1}\Delta\text{CD4}+\text{LL}/2} = 11$ ; Spleen:  $N_{\text{NFATc1}^{\text{fl/fl}}+\text{LL}/2} = 4$ ,  $N_{\text{NFATc1}\Delta\text{CD4}+\text{LL}/2} = 5$ ). **e-g**, Flow cytometry analysis of  $\text{CD8}^+$  memory T-cells in the spleen and the lung of tumour-bearing  $\text{NFATc1}^{\text{fl/fl}}$  and  $\text{NFATc1}^{\Delta\text{CD4}}$  mice. Percentage of  $\text{CCR7}^+\text{CD62L}^+\text{CD8}^+$  (%) central memory T-cells (TCM) and  $\text{CCR7}^-\text{CD62L}^-\text{CD8}^+$  (%) effector memory T-cells (TEM) in total cell suspension of the spleen **e**, ( $N_{\text{NFATc1}^{\text{fl/fl}}+\text{LL}/2} = 3$ ,  $N_{\text{NFATc1}\Delta\text{CD4}+\text{LL}/2} = 3$ ). Percentage of  $\text{Ly6C}^+\text{KLRG1}^+\text{CD62L}^-\text{CD8}^+$  (%) TEM cells **f**, and  $\text{CD103}^+\text{CD8}^+$  (%) tissue-resident memory T-cells (TRM) **g**, in total cell suspension of the lung ( $N_{\text{NFATc1}^{\text{fl/fl}}+\text{LL}/2} = 4$ ,  $N_{\text{NFATc1}\Delta\text{CD4}+\text{LL}/2} = 5$ ). N values are given per group. Data are shown as mean values  $\pm$  s.e.m. using student's two-tailed t-test \*P,0.05; \*\*P,0.01, \*\*\*P,0.001.

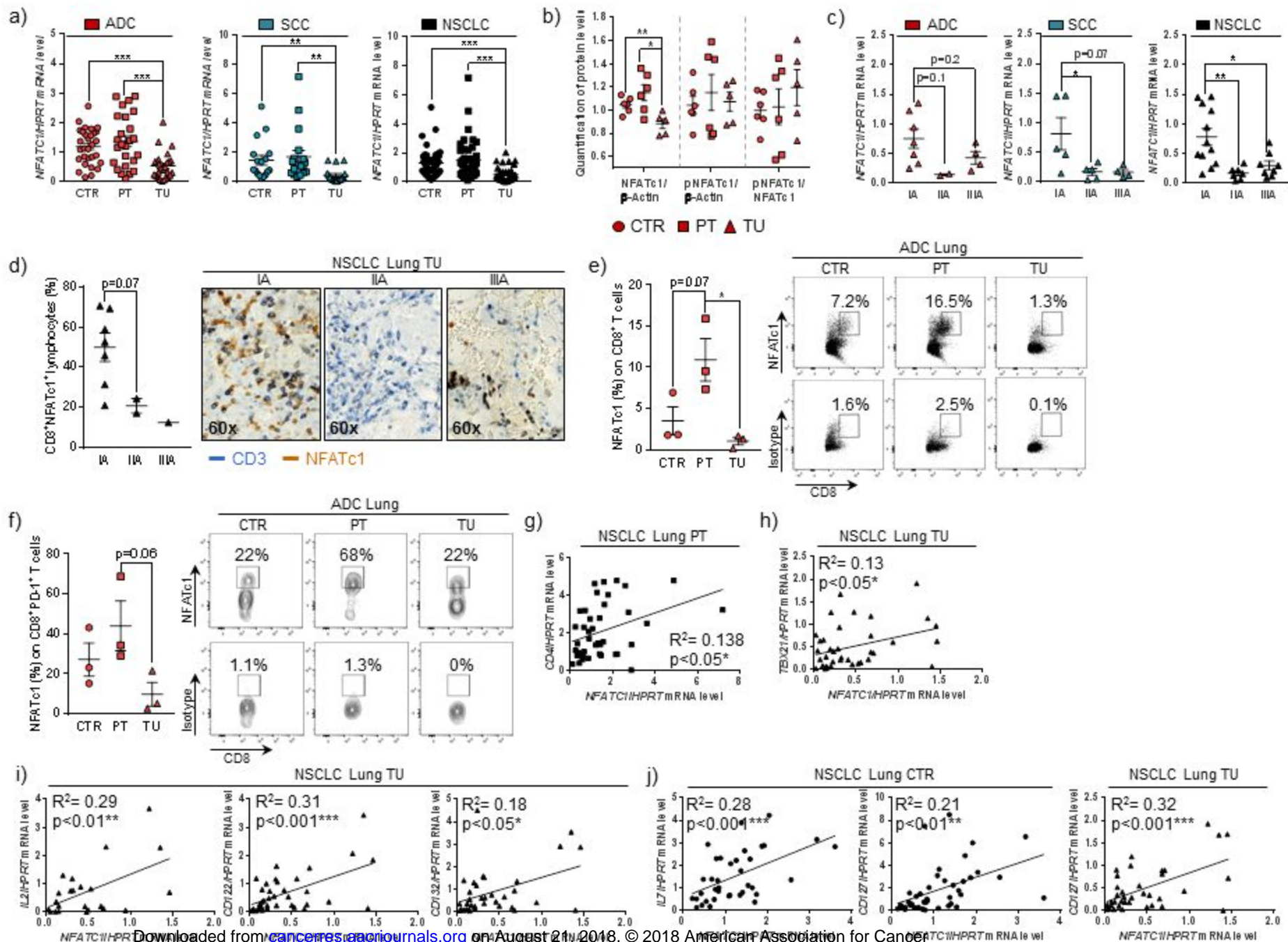
**Figure 5: Cytokines secreted from NFATc1<sup>ΔCD4</sup> dLNs support tumour cell growth.**

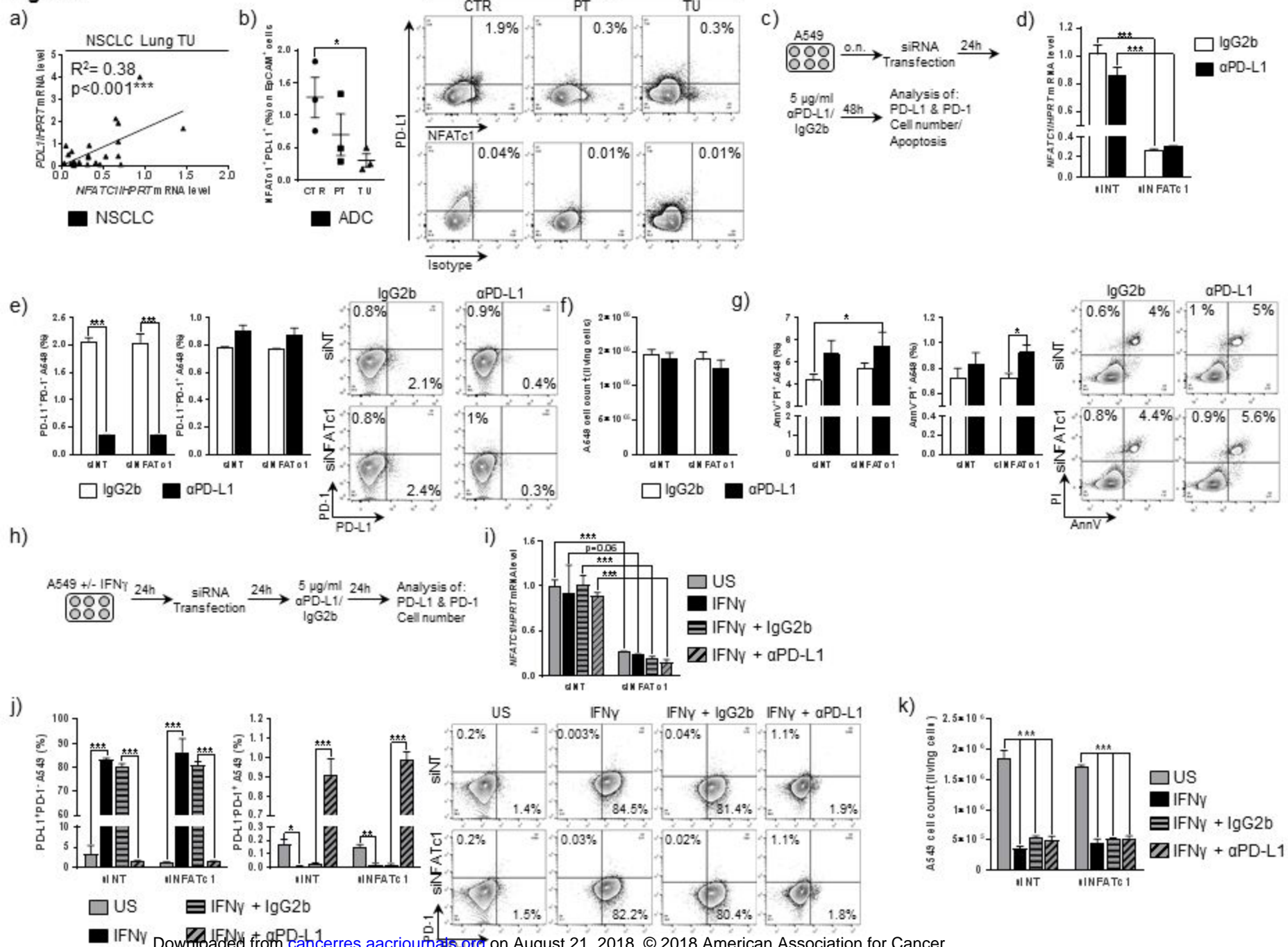
**a**, Flow cytometry analysis of CD25 expressing CD4<sup>+</sup> T-cells (%) in total lung cell suspension of lung tumour-bearing NFATc1<sup>fl/fl</sup> and NFATc1<sup>ΔCD4</sup> mice ( $N_{\text{NFATc1fl/fl+LL/2}} = 8$ ,  $N_{\text{NFATc1ΔCD4+LL/2}} = 11$ ). **b**, Flow cytometry analysis of IL-2 production by CD4<sup>+</sup> T-cells (%) in total cell suspension of the lung and the spleen of tumour-bearing NFATc1<sup>fl/fl</sup> and NFATc1<sup>ΔCD4</sup> mice (Lung:  $N_{\text{NFATc1fl/fl+LL/2}} = 8$ ,  $N_{\text{NFATc1ΔCD4+LL/2}} = 11$ ; Spleen:  $N_{\text{NFATc1fl/fl+LL/2}} = 4$ ,  $N_{\text{NFATc1ΔCD4+LL/2}} = 5$ ). **c**, Flow cytometry analyses of CD4<sup>+</sup> T-cell population (%) in total cell suspension of the spleen and the draining lymph nodes (dLN) of tumour-bearing NFATc1<sup>fl/fl</sup> and NFATc1<sup>ΔCD4</sup> mice (Spleen:  $N_{\text{NFATc1fl/fl+LL/2}} = 4$ ,  $N_{\text{NFATc1ΔCD4+LL/2}} = 5$ ; dLN:  $N_{\text{NFATc1fl/fl+LL/2}} = 8$ ,  $N_{\text{NFATc1ΔCD4+LL/2}} = 10$ ). **d**, Flow cytometry analysis of PD-1 (%) gated on CD4<sup>+</sup>ICOS<sup>+</sup> T-cells in total cell suspension of dLN of tumour-bearing NFATc1<sup>fl/fl</sup> and NFATc1<sup>ΔCD4</sup> mice ( $N_{\text{NFATc1fl/fl+LL/2}} = 8$ ,  $N_{\text{NFATc1ΔCD4+LL/2}} = 9$ ). **e**, Experimental design: cytotoxicity assay of LL/2 cells incubated with lymph node-conditioned medium (LNCM) from dLNs of tumour-bearing mice. Total cells of dLNs were cultured for 24h in the presence of αCD3 and αCD28 antibodies and resulting supernatant (SN) was defined as LNCM. LL/2 cells were incubated with 20% LNCM for 24h followed by luminescence analysis to determine LL/2 cell numbers. **f**, Results of LL/2 cytotoxicity assay. LL/2 cells were incubated with 20% LNCM of tumour-bearing NFATc1<sup>fl/fl</sup> and NFATc1<sup>ΔCD4</sup> mice. RPMI medium was used as a negative control, SN of CTLL2 cells as a positive control ( $N_{\text{NFATc1fl/fl+LL/2}} = 7$ ,  $N_{\text{NFATc1ΔCD4+LL/2}} = 10$ ,  $N_{\text{RPMI}} = 8$ ,  $N_{\text{CTLL2}} = 7$ ). **g-i**, ELISA analysis of TNFα **g**, IL-2 **h**, and IL-7 **i**, levels in LNCM of lung tumour-bearing NFATc1<sup>fl/fl</sup> and NFATc1<sup>ΔCD4</sup> mice (TNFα:  $N_{\text{NFATc1fl/fl+LL/2}} = 6$ ,  $N_{\text{NFATc1ΔCD4+LL/2}} = 10$ ; IL-2:  $N_{\text{NFATc1fl/fl+LL/2}} = 3$ ,  $N_{\text{NFATc1ΔCD4+LL/2}} = 6$ ; IL-7:  $N_{\text{NFATc1fl/fl+LL/2}} = 3$ ,  $N_{\text{NFATc1ΔCD4+LL/2}} = 5$ ). **j**, LL/2 cells were cultured in the presence or absence (CTR) of TNFα (30 ng/ml) for 0-48 h and treated with the IncuCyte Caspase-3/7 reagent to detect apoptotic cells (green object count, 1/mm<sup>2</sup>) using the IncuCyte live-cell analysis system ( $N_{\text{CTR}} = 3$ ,

$N_{TNF\alpha}=3$ ). N values are given per group. Data are shown as mean values  $\pm$  s.e.m. using student's two-tailed t-test \*P,0.05; \*\*P,0.01, \*\*\*P,0.001.

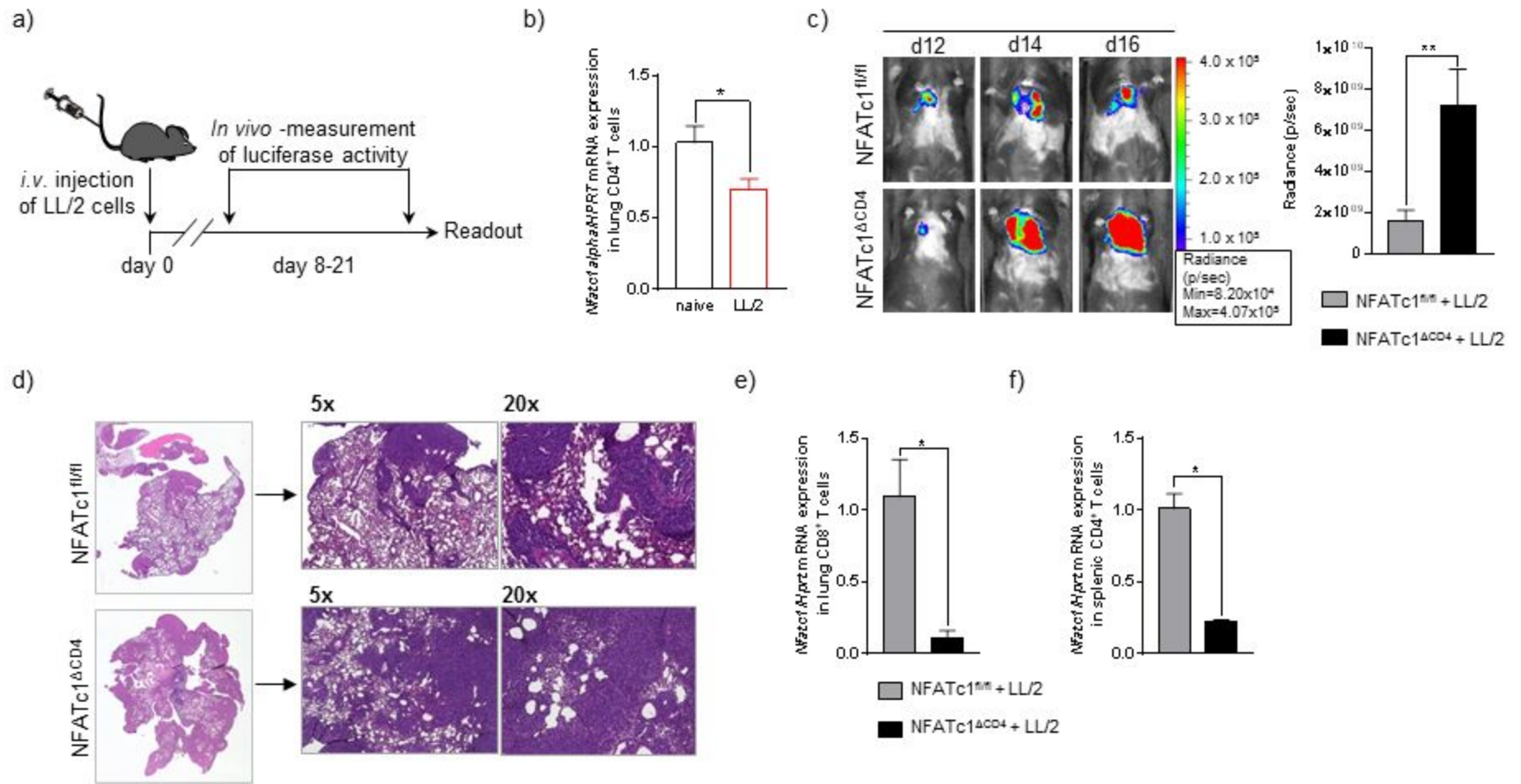
**Figure 6:  $\alpha$ PD-1 antibody treatment induced NFATc1 in CD4<sup>+</sup> and CD8<sup>+</sup> T-cells.**

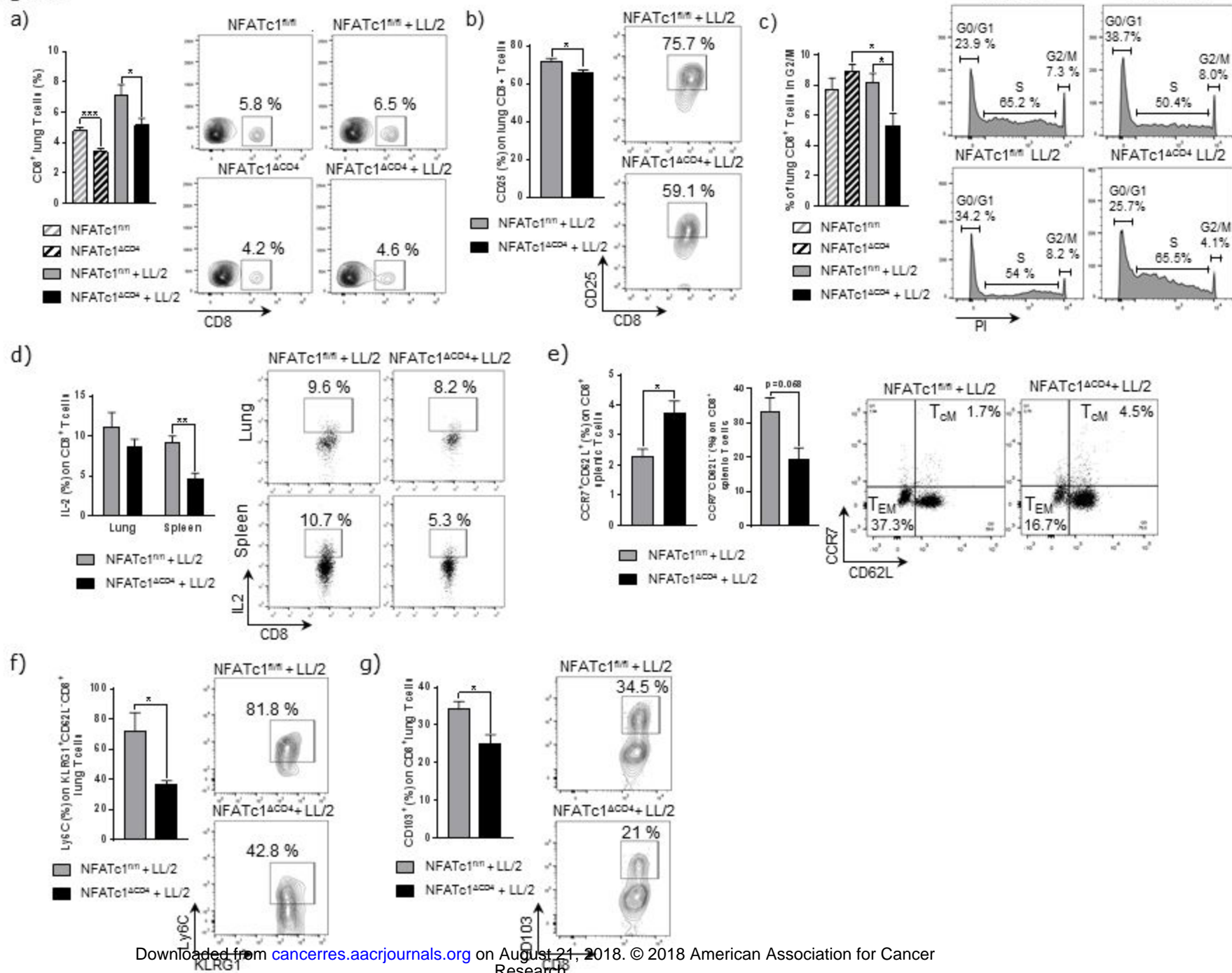
**a**, Experimental design: Lung tumour growth was induced via intravenous (i.v.) injection of LL/2-luc-M38 (LL/2) lung carcinoma cells in C57BL/6 wild-type (WT) mice. At day 9, 12, 15 and 18 post injection mice were treated intraperitoneally (i.p.) with  $\alpha$ PD-1 antibody or IgG2a isotype control and tumour load was analyzed via an *in vivo* bioluminescence based imaging system. At day 20 post injection total lung cells were *in vitro* re-challenged with  $\alpha$ PD-1 and IgG2a antibodies for 24h. **b**, Overall survival rate (%); **c**, Weight change (%) and **d**, Radiance (photon flux/second) of C57BL/6 WT mice *in vivo* treated with  $\alpha$ PD-1 or IgG2a antibodies (Day9-18  $N_{IgG2a}=5$ ,  $N_{\alpha PD-1}=5$ ; day18-20  $N_{IgG2a}=4$ ,  $N_{\alpha PD-1}=4$ ). **e-f**, Total lung cell suspension of C57BL/6 WT mice *in vivo* treated with  $\alpha$ PD-1 or IgG2a antibodies were *in vitro* re-challenged with  $\alpha$ PD-1 or IgG2a antibodies or left unstimulated (US). Flow cytometry analyses of NFATc1 in CD4<sup>+</sup> T-cells (%) **e**, and NFATc1 in CD8<sup>+</sup> T-cells (%) **f**, (US<sup>*In vitro*</sup>:  $N_{IgG2a}=3$ ,  $N_{\alpha PD-1}=3$ ; IgG2a<sup>*In vitro*</sup>:  $N_{IgG2a}=3$ ,  $N_{\alpha PD-1}=3$ ;  $\alpha$ PD-1<sup>*In vitro*</sup>:  $N_{IgG2a}=3$ ,  $N_{\alpha PD-1}=3$ ). **g**, Experimental design: cytotoxicity assay of LL/2 cells incubated with supernatant from total lung cells (= lung-conditioned medium, LUCM) of C57BL/6 WT mice *in vivo* treated with  $\alpha$ PD-1 or IgG2a and *in vitro* re-challenged with  $\alpha$ PD-1 or IgG2a antibodies or left unstimulated (US). LL/2 cells were incubated with 20% LUCM for 24h followed by luminescence analysis to determine LL/2 cell numbers. **h**, Results of LL/2 cytotoxicity assay. Supernatant of CTLL2 cells was used as a positive control (US<sup>*In vitro*</sup>:  $N_{IgG2a}=4$ ,  $N_{\alpha PD-1}=4$ ; IgG2a<sup>*In vitro*</sup>:  $N_{IgG2a}=4$ ,  $N_{\alpha PD-1}=4$ ;  $\alpha$ PD-1<sup>*In vitro*</sup>:  $N_{IgG2a}=4$ ,  $N_{\alpha PD-1}=4$ ; CTLL2:  $N=3$ ). N values are given per group. Data are shown as mean values  $\pm$  s.e.m. using student's two-tailed t-test \*P,0.05; \*\*P,0.01, \*\*\*P,0.001.

**Figure 1**

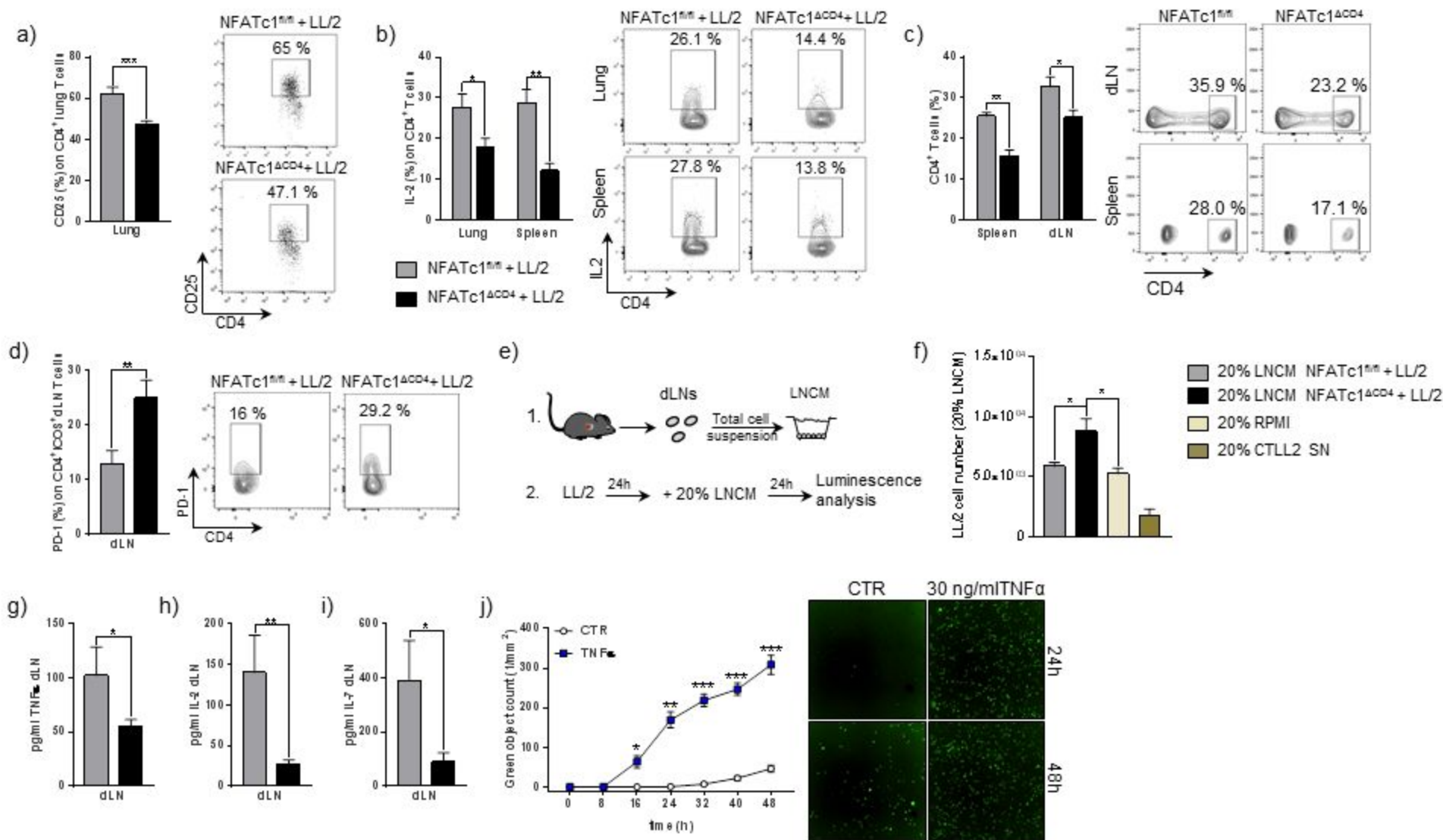
**Figure 2**

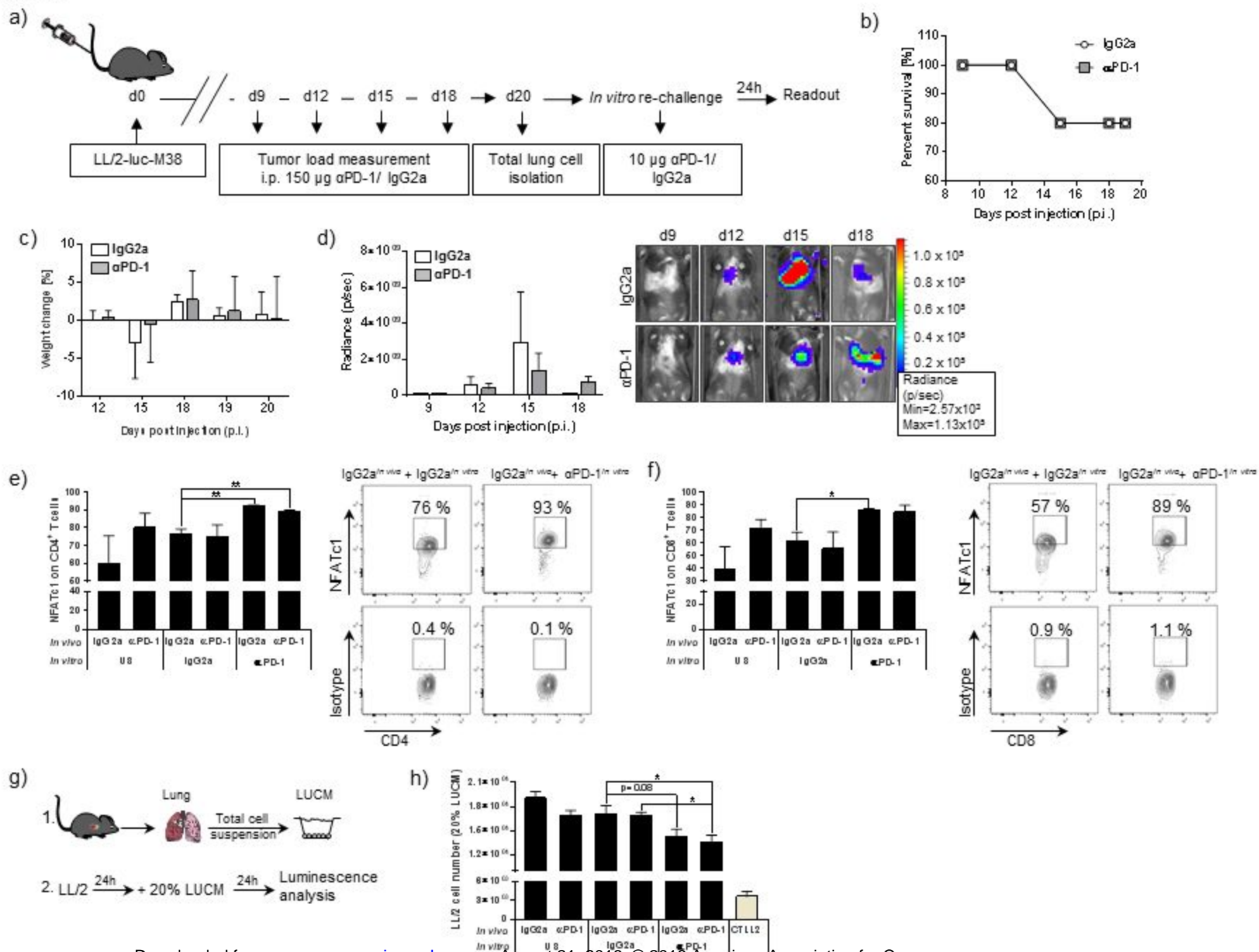
**Figure 3**



**Figure 4**

**Figure 5**



**Figure 6**

# Cancer Research

The Journal of Cancer Research (1916–1930) | The American Journal of Cancer (1931–1940)

## NFATc1 promotes anti-tumoral effector functions and memory CD8+ T cell differentiation during non-small cell lung cancer development

Lisanne Heim, Juliane Friedrich, Marina Engelhardt, et al.

*Cancer Res* Published OnlineFirst April 24, 2018.

<b>Updated version</b>	Access the most recent version of this article at: doi: <a href="https://doi.org/10.1158/0008-5472.CAN-17-3297">10.1158/0008-5472.CAN-17-3297</a>
<b>Supplementary Material</b>	Access the most recent supplemental material at: <a href="http://cancerres.aacrjournals.org/content/suppl/2018/04/24/0008-5472.CAN-17-3297.DC1">http://cancerres.aacrjournals.org/content/suppl/2018/04/24/0008-5472.CAN-17-3297.DC1</a>
<b>Author Manuscript</b>	Author manuscripts have been peer reviewed and accepted for publication but have not yet been edited.

<b>E-mail alerts</b>	<a href="#">Sign up to receive free email-alerts</a> related to this article or journal.
<b>Reprints and Subscriptions</b>	To order reprints of this article or to subscribe to the journal, contact the AACR Publications Department at <a href="mailto:pubs@aacr.org">pubs@aacr.org</a> .
<b>Permissions</b>	To request permission to re-use all or part of this article, use this link <a href="http://cancerres.aacrjournals.org/content/early/2018/04/24/0008-5472.CAN-17-3297">http://cancerres.aacrjournals.org/content/early/2018/04/24/0008-5472.CAN-17-3297</a> . Click on "Request Permissions" which will take you to the Copyright Clearance Center's (CCC) Rightslink site.